

Integration of Preferences in Decomposition Multi-Objective Optimisation*

Ke Li^{#1}, Renzhi Chen^{#2}, Geyong Min¹ and Xin Yao^{2,3}

¹Department of Computer Science, University of Exeter

²Department of Computer Science and Engineering, Southern University of Science and Technology

³CERCIA, School of Computer Science, University of Birmingham

⁴Department of Engineering, University of Exeter

*Email: {k.li, g.min}@exeter.ac.uk, rxc332@cs.bham.ac.uk, xiny@sustc.edu.cn

#The first two authors make equal contributions to this paper.

Abstract: Most existing studies on evolutionary multi-objective optimisation focus on approximating the whole Pareto-optimal front. Nevertheless, rather than the whole front, which demands for too many points (especially in a high-dimensional space), the decision maker might only interest in a partial region, called the region of interest. In this case, solutions outside this region can be noisy to the decision making procedure. Even worse, there is no guarantee that we can find the preferred solutions when tackling problems with complicated properties or a large number of objectives. In this paper, we develop a systematic way to incorporate the decision maker's preference information into the decomposition-based evolutionary multi-objective optimisation methods. Generally speaking, our basic idea is a non-uniform mapping scheme by which the originally uniformly distributed reference points on a canonical simplex can be mapped to the new positions close to the aspiration level vector specified by the decision maker. By these means, we are able to steer the search process towards the region of interest either directly or in an interactive manner and also handle a large number of objectives. In the meanwhile, the boundary solutions can be approximated given the decision maker's requirements. Furthermore, the extent of the region of the interest is intuitively understandable and controllable in a closed form. Extensive experiments, both proof-of-principle and on a variety of problems with 3 to 10 objectives, fully demonstrate the effectiveness of our proposed method for approximating the preferred solutions in the region of interest.

Keywords: Evolutionary multi-objective optimisation, decomposition-based method, user-preference incorporation, reference points.

1 Introduction

Many real-life applications usually consider optimising multiple conflicting objectives simultaneously. To handle such problems, termed as multi-objective optimisation problems (MOPs), decision makers (DMs) often look for a set of Pareto-optimal solutions none of which can be considered better than another when all objectives are of importance. Evolutionary multi-objective optimisation (EMO) algorithms, which work with a population of solutions and can approximate a set of trade-off alternatives simultaneously, have been widely accepted as a major tool for solving MOPs. Over the past two decades and beyond, many efforts have been devoted to developing EMO algorithms (e.g. elitist non-dominated sorting genetic algorithm (NSGA-II) [1] and its variants [2–4], indicator-based EA (IBEA) [5] and multi-objective EA based on decomposition (MOEA/D) [6]) to find a set of efficient solutions that well approximate the whole Pareto-optimal front (PF) in terms of convergence and diversity.

The ultimate goal of multi-objective optimisation is to help the DM find solutions that meet at most his/her preferences. Supplying a DM with a large amount of trade-off points, which approximate the whole PF, not only increases his/her workload, but also provides many irrelevant or even

*This article is accepted for publication in IEEE Transactions on Cybernetics. Copy right is transferred to IEEE while this is a manuscript version.

noisy information to the decision-making procedure. Moreover, due to the curse of dimensionality, approximating a high-dimensional PF as a whole not only becomes computationally inefficient (or even infeasible), but also causes a severe cognitive obstacle for the DM to comprehend the high-dimensional data. To facilitate the decision-making procedure, it is more practical to incorporate the DM’s preference information into the search process. This allows the computational efforts to concentrate on the region of interest (ROI) and thus has a better approximation therein. In general, the preference information can be incorporated *a priori*, *posteriori* or *interactively*. Note that the traditional EMO goes along the posteriori way of which the disadvantages have been discussed before. If the preference information is elicited a priori, it is directly used to guide the solutions toward the ROI. However, it is non-trivial to faithfully model the preference information before solving the MOP at hand. Eliciting the preference information in an interactive manner has been studied in the multi-criterion decision-making (MCDM) field for over half a century. It enables the DM to progressively learn and understand the characteristics of the MOP at hand and adjust his/her elicited preference information. Consequently, solutions are effectively driven toward the ROI. However, since the optimisation process is full of uncertainty and the DM is almost unavoidable to show inconsistencies in decision-making [7], it is difficult to model the DM’s behaviour in an appropriate manner.

Integrating and blending the EMO and MCDM together to tailor the DM’s preference information has been studied since 90’s [8–11]. Although the existing works aim at steering the search process toward the ROI, the definition of the ROI is still vague. First of all, the ROI can be any part of the PF near the DM supplied aspiration level vector or even subjectively determined by the DM. Secondly, the ROI is expected to be a partial region of the PF whereas no quantitative definition has been given to the size of this region. Although some studies (e.g. [12–14]) claimed to control the spread of the preferred solutions accommodating to the DM’s expectation of the extent of the ROI, i.e. the ROI’s size, the corresponding parameter setting is ad-hoc [11]. In addition to the ROI, the boundary of the PF is also important for the DM to understand the underlying problem and to facilitate the further decision-making procedure. In particular, the boundary provides the DM general information about the PF’s geometrical characteristics; and more importantly, it provides the information of the ideal and nadir points which facilitate the normalisation of the disparately scaled objective functions. Unfortunately, how to keep solutions located in the ROI and the boundary simultaneously has rarely been studied [15].

During recent years, especially after the developments of MOEA/D and NSGA-III [16], the decomposition-based EMO methods have become increasingly popular for the posteriori multi-objective optimisation. Generally speaking, by specifying a set of reference points¹, the decomposition-based EMO methods at first decompose the MOP at hand into multiple subproblems, either with scalar objective or simplified multi-objective. Then, a population-based technique is applied to solve these subproblems in a collaborative manner. Under some mild conditions, the optimal solutions of all subproblems constitute a good approximation to the PF. It is not difficult to understand that the distribution of the reference points is essential in a decomposition-based EMO method. It not only implies a priori prediction of the PF’s geometrical characteristics, but also determines the distribution of Pareto-optimal solutions. [17] and [18] suggested some structured methods to generate evenly distributed reference points on a canonical simplex. To adapt to the irregular PFs, such as disconnected or mixed shapes and disparately scaled objectives, some adaptive reference point adjustment methods (e.g. [19] and [20]) have been developed to adjust the distribution of reference points on the fly. To integrate the DM’s preference information into the decomposition-based EMO methods, a natural idea is to make the distribution of the reference points be biased toward the ROI. Although it sounds intuitive, in practice, how to obtain the appropriate reference points that accommodate to the DM’s preference information is far from trivial. Most recently, there have been some initiatives on adjusting the distribution of the reference points according to the DM’s preference information (e.g. [21–23]). However, they are ad-hoc and the position and extent of the reference points around the ROI are not fully controllable.

In this paper, we present a systematic way to incorporate the DM’s preference information, either a

¹In this paper, we use the term reference point without loss of generality, although some other literatures, e.g. the original MOEA/D [6], also use the term weight vector interchangeably.

priori or interactively, into the decomposition-based EMO methods. In particular, the DM’s preference information is modelled as an aspiration level vector, which has been widely used in the EMO literature [11]. Comparing to three state-of-the-art preference-based EMO algorithms, the effectiveness and competitiveness of the proposed preference incorporation method for assisting three state-of-the-art decomposition-based EMO algorithms to approximate ROIs have been validated through extensive experiments on 56 test problems with 2 to 10 objectives, under both attainable and unattainable aspiration level vector settings. Our major contributions are outlined as follows.

- Our basic idea is a non-uniform mapping scheme by which the originally evenly distributed reference points on a canonical simplex can be mapped to new positions close to the DM specified aspiration level vector and thereby having a biased distribution.
- The mapping function is nonlinear in nature and is a function of a reference point’s position with respect to the pivot point. Accordingly, the distribution of the reference points after the non-uniform mapping is biased toward the pivot point. In particular, this pivot point is the representative of the ROI on the simplex and determines the ROI’s position.
- Different from the existing preference-based EMO algorithms, where the extent of the approximated ROI is controlled in an ad-hoc manner, this paper provides an intuitively understandable manner to quantify this extent in a closed form. It is the ratio of the biased reference points proportional to the simplex. To a certain extent, this quantity can be used as the ratio of the ROI’s size with respect to the PF.
- Given the DM’s requirements, the proposed non-uniform mapping scheme is able to not only obtain a set of biased reference points toward the ROI, but also preserve the ones located on the boundary. This latter characteristic enables a decomposition-based EMO method not only find the preferred solutions, but also provide the global information about the PF to the DM.

The rest of this paper is organised as follows. Section 2 devotes to overviewing some state-of-the-art related to this paper. Section 3 presents the technical details of our proposed non-uniform mapping scheme. Section 4 and Section 5 show the empirical studies on several benchmark problems. Finally, Section 6 provides some concluding remarks along with some future directions.

2 Related Works

In the past two decades, various methods have been developed to incorporate the DM’s preference information into the EMO. This section briefly overviews the existing literature according to the ways of eliciting the DM’s preference information along with the mechanisms adopted to guide the population toward the ROI. The interested reader is referred to [8–11] for the more comprehensive survey.

The first one employs the weight information, i.e. relative importance, to model the DM’s preference information. For example, Deb et al. [24] developed a modified fitness sharing mechanism, by using a weighted Euclidean distance, to bias the population distribution. Branke and Deb [25] developed a weighted mapping method to modify the crowding distance calculation of NSGA-II by which the search process can be guided toward the ROI. Note that the weight-based methods become ineffective when facing a large number of objectives. Because it is difficult to either specify the weights or verify the quality of the biased approximation. Moreover, it is unintuitive and challenging for the DM to steer the search process toward the ROI via the weighting scheme.

The second sort elicits the preference information by inviting the DM to make pairwise comparisons among a sample of solutions from a population. As the pioneer, Phelps and Köksalan [26] proposed to use a value function model to represent the DM’s preference information. Note that the precise form of the value function model is unknown a priori. It is progressively learned through a periodic interaction with the DM during the optimization process. In particular, the DM is asked to express his/her preference information about some selected alternatives, e.g. their rankings, at each interaction session. Inspired by [26], many variants have been developed by using various value function models,

e.g. quasi-concave preference function [27], polynomial value function [28], support vector machine [29] and ordinal regression [30]. In [31], Gong et al. proposed to use a preference polyhedron to approximate the DM's value function by choosing the best and worst solutions from the current non-dominated solutions. In [32], Parmee and Cvetkovic suggested a method to integrate the DM's fuzzy preference information into the EMO algorithm by converting the linguistic terms into weights. This sort of methods are interesting but complicated, especially when the number of objectives becomes large. In addition, using such an approach interactively increases the DM's cognitive load and it is hard to control the extent of the ROI. In [15], the biased distribution of solutions is achieved by setting different territory sizes in the territory-based evolutionary algorithm [33]. In particular, a smaller territory leads to a higher resolution of solutions, and vice versa. The size of the corresponding territory is progressively adjusted by the interaction with the DM. Note that this work is one of the few that acknowledged the importance of providing information on the extent of the solution space while converging the ROI. The major drawback of this method comes from its diversity management, especially in a high-dimensional space. Due to the same reason, it might be difficult to control the extent of the ROI precisely.

The third category transforms the DM's preference information into some modified trade-off relationship to compare solutions [34]. In [35], Greenwood et al. suggested an imprecisely specified multi-attribute utility theory-based weighted sum method to obtain the ranking of objectives from some candidate solutions.

The fourth category [36] invites the DM to express his/her preference information by supplying two thresholds: an absolutely satisfying objective value and a marginally infeasible objective value. Afterwards, each objective function of the original MOP is converted into a desirability function by using these thresholds as parameters. Then, an EMO algorithm is applied to optimise the desirability functions instead of the original objective functions.

The fifth class [37,38] uses outranking concept [39] to incorporate the DM's preference information. Specifically, by specifying some necessary parameters, a DM develops a fuzzy predicate that models the truth degree of the predicate "solution \mathbf{x} is at least as good as solution \mathbf{y} ".

The last one uses aspiration level vectors to represent the DM's desired values/levels for each objective he/she would like to achieve. As the first attempt, Fonseca and Fleming [40] suggested to model the DM's preference as a goal, i.e. the aspiration level vector, to achieve. In [12,41] and [42], Deb et al. combined the reference point, i.e. aspiration level vector, related methods with NSGA-II to guide the search process toward the ROI. In particular, solutions close to the given reference point have a high priority to survive to the next generation. In [43] and [44], the aspiration level vector is used to help select the leader swarm in the multi-objective particle swarm optimisation algorithm. Molina et al. [45] suggested a modified dominance relationship, called g-dominance, where solutions satisfying either all or none aspiration levels are preferred over those satisfying some aspiration levels. Said et al. [13] developed another modified dominance relationship, called r-dominance, where non-dominated solutions, according to the Pareto dominance relationship, can be distinguished by their weighted Euclidean distances toward the DM supplied aspiration level vector. Recently, some decomposition-based methods also used the aspiration level vector to incorporate the DM's preference information into the search process, e.g. [23] and [46–48]. Their basic idea is to use the aspiration level vector as the anchor around which they try to obtain some reference points. Although, by specifying aspiration level vectors, a DM is able to guide the search toward the ROI directly or interactively even when encountering a large number of objectives, existing methods cannot approximate the solutions in the ROI and the boundary simultaneously. In addition, the control of the extent of the ROI is ad-hoc.

3 Non-Uniform Mapping Scheme

3.1 Overview

Reference points, as the basic components in the decomposition-based EMO algorithms, are usually generated in a structured manner, e.g. the Das and Dennis's method² [17]. Fig. 1(a) shows an example of 91 evenly distributed reference points in a three-dimensional space. In this case, the DM has no preference on any particular region of the PF. These reference points are used to guide a decomposition-based EMO algorithm search for the whole PF. On the other hand, if the DM has elicited some preference information, e.g. an aspiration level vector, it is preferable that reference points can have a biased distribution toward the ROI accordingly. Bearing this consideration in mind, this section presents a non-uniform mapping scheme (NUMS) by which we are able to change the originally evenly distributed reference points to be biased toward the ROI. Fig. 1(b) and Fig. 1(c) show two examples of the biased reference points distribution after the non-uniform mapping. In the following paragraphs, we will describe the mathematical model of the NUMS in detail before showing its algorithmic implementations.

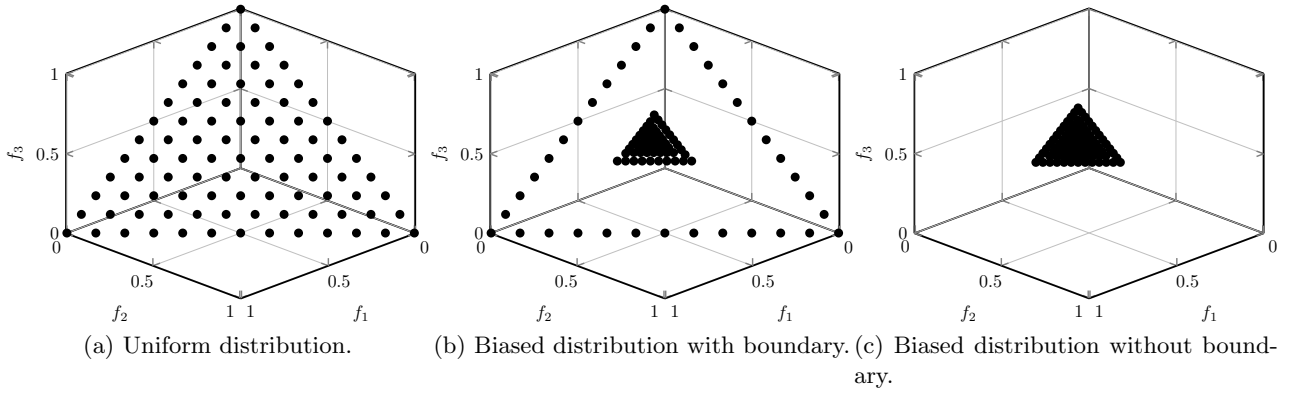


Figure 1: Reference points used in decomposition-based EMO methods.

3.2 NUMS in One-Dimensional Space

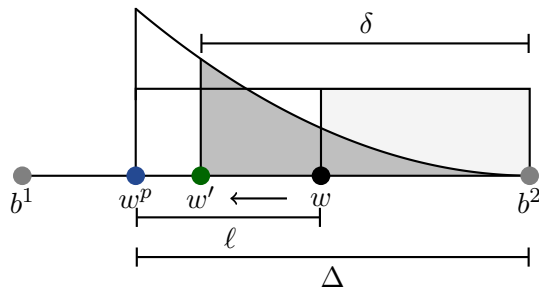


Figure 2: Non-uniform mapping scheme in 1-D scenario.

Let us start with a one-dimensional case. Considering the illustrative example shown in Fig. 2, the reference points generated in a structured manner are evenly distributed along the line starting from b^1 and ending at b^2 . Let us assume that the position of an evenly distributed reference point w obeys a uniform distribution whose probability density function (PDF) is defined as follows:

$$\psi^u(\zeta) = \frac{1}{\Delta} \quad (1)$$

²In [17], $N = \binom{H+m-1}{m-1}$ reference points, with a uniform spacing $\delta = \frac{1}{H}$, are sampled from a canonical simplex Ψ^m , where $H > 0$ is the number of divisions considered along each objective coordinate, and m is the number of objectives.

where $\|\cdot\|$ represents ℓ^2 -norm and ρ is calculated as:

$$\rho = \Delta - \delta \quad (7)$$

where $\Delta = \|\mathbf{b} - \mathbf{w}^p\|$ and δ is calculated based on equation (5) in which $\ell = \|\mathbf{w} - \mathbf{w}^p\|$. Note that \mathbf{w} and \mathbf{w}^p are known a priori, while \mathbf{b} is one of the intersecting points between the line connecting \mathbf{w}^p and \mathbf{w} and the edges of the simplex Ψ^m . Generally speaking, \mathbf{b} can be calculated as:

$$\mathbf{b} = \mathbf{w}^p + \Delta \times \frac{\mathbf{w} - \mathbf{w}^p}{\|\mathbf{w} - \mathbf{w}^p\|} \quad (8)$$

Geometrically, there are at most m such intersecting points, each of which should have a zero element. In this case, for each \mathbf{b}^i , $i \in \{1, \dots, m\}$, the corresponding Δ in equation (8) can be calculated as:

$$\Delta = \min_{1 \leq i \leq m} [w_i^p \times \frac{\|\mathbf{w}^p - \mathbf{w}\|}{w_i^p - w_i}]_+ \quad (9)$$

where $[\sigma]_+$ returns σ if and only if $\sigma > 0$, otherwise it returns an invalid number.

3.4 Effects and Setting of η

Fig. 4 shows six function curves with various η settings. From this figure, we can infer that η controls the gradient of the PDF curve. $\psi^e(\xi)$ is a decreasing function of ξ when $\eta > 0$; while it is an increasing function of ξ when $\eta < 0$. From Fig. 4, we also find that the function curve is more skewed with a larger η . According to the properties of power function, it is not difficult to understand that, for a given Δ and ℓ in equation (5), a larger η will result in a larger δ . In summary, η has the following two effects on the NUMS:

- To push \mathbf{w} toward \mathbf{w}^p , we need to set $\eta > 0$; otherwise \mathbf{w} will be shifted away from \mathbf{w}^p .
- With a large η , which results in a large δ , \mathbf{w}' has a large probability to be closer to \mathbf{w}^p after the non-uniform mapping; on the flip side, \mathbf{w}' will be closer to \mathbf{b} .

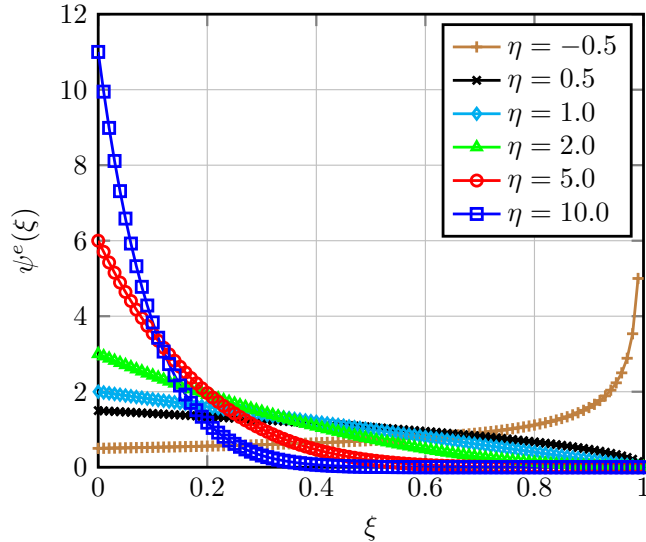


Figure 4: The shape of $\psi^e(\xi)$ with different η .

Based on the above discussions, we realise that η is able to control the extent of the biased reference points after the non-uniform mapping. However, due to the non-linear property of the PDF in equation (2), it is far from trivial to choose the appropriate η beforehand that results in the expected extent of the ROI. Instead of tweaking η , by trial-and-error, with respect to the non-linear mapping function, here we introduce an intuitively understandable way to control the extent of the ROI. Specifically, rather than a concrete extent of the ROI, it is more plausible for the DM to specify

a relative quantity in practice. Here we use τ ($0 < \tau \leq 1$), the ratio of the surface area of the biased reference points proportional to the simplex Ψ^m , as this quantity. As discussed in [6], under certain smoothness assumption, each reference point is supposed to correspond to a Pareto-optimal solution. Therefore, τ can also be regarded as an relative ratio of the ROI's size with respect to the PF. Given τ , collected as an additional preference information elicited by the DM, Theorem 1 gives a closed form for setting the corresponding η value.

Theorem 1. *Given the relative extent τ ($0 < \tau \leq 1$) of reference points after the non-uniform mapping, comparing to the simplex Ψ^m , the η value in equation (2) is calculated as*

$$\eta = \frac{\log \alpha}{\log \beta} - 1 \quad (10)$$

where $\alpha = \frac{m}{H}$ and $\beta = 1 - \tau$.

The proof of Theorem 1 can be found in Appendix A of the supplementary document³. Fig. 5 shows three examples of biased reference points after the non-uniform mapping with different τ settings. Based on Theorem 1, we have the following corollary which provides the upper and lower bounds for setting τ .

Corollary 1. *To make the extent of the biased reference points shrink, we need to set $0 < \tau < 1 - \frac{m}{H}$.*

The proof of Corollary 1 can be found in Appendix B of the supplementary document. In principle, comparing to the whole PF, the relative extent of the ROI can be any number between 0 and 1. However, Corollary 1 provides a restriction on τ in order to make the evenly distributed reference points shrink to the ROI; otherwise they will expand toward the boundary. It is worth noting that Theorem 1 and Corollary 1 are derived under the condition $H > m$. Otherwise, all reference points generated by the Das and Dennis's method should lie on the boundary of the simplex Ψ^m . How to shift the reference points lying on the boundary will be described in the next subsection.

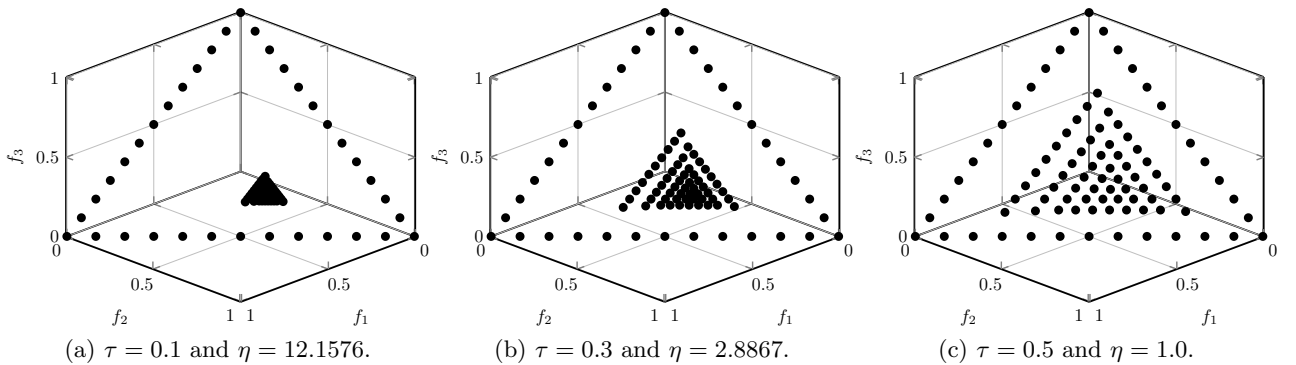


Figure 5: Distribution of reference points for different settings of τ and their corresponding η when $\mathbf{z}^r = (0.7, 0.8, 0.5)^T$.

3.5 Boundary Preservation

Note that the NUMS described so far shifts the reference points, except those lying on the boundary of the simplex Ψ^m , onto the ROI. The biased reference points try to guide a decomposition-based EMO algorithm not only search for the preferred solutions, but also approximate those lying on the PF's boundary. In particular, the boundary solutions provide the DM more comprehension of the PF, e.g. the PF's general shape, the ideal and nadir points which can be useful for further decision-making. Nevertheless, if the DM is not interested in the boundary any longer, we can make a simple modification on the NUMS to shift the reference points lying on the boundary toward the ROI as

³The supplementary document can be found in <https://coda-group.github.io/supp.pdf>

well. Specifically, a reference point \mathbf{w}^b is considered lying on the boundary of Ψ^m if and only if the following condition is met:

$$\Delta - \|\mathbf{w}^b - \mathbf{w}^p\| < \epsilon \quad (11)$$

where $\epsilon = 10^{-6}$ is a small quantity and Δ is determined according to equation (9). To shift \mathbf{w}^b onto the ROI, its new position after the NUMS is calculated as:

$$\mathbf{w}' = \mathbf{w}^p + \rho \times \frac{\mathbf{w}^b - \mathbf{w}^p}{\|\mathbf{w}^b - \mathbf{w}^p\|} \quad (12)$$

where $\rho = \tau \times \|\mathbf{w}^b - \mathbf{w}^p\|$. Note that the η value derived in Theorem 1 is under the consideration that the DM is willing to keep the boundary points. If the reference points lying on the boundary are shifted onto the ROI by the NUMS as well, the η value should be calculated according to Corollary 2.

Corollary 2. *If all reference points are shifted onto the ROI, the η value in equation (2) is calculated as:*

$$\eta = \frac{\log \alpha}{\log \beta} - 1 \quad (13)$$

where $\alpha = \frac{m}{H}$ and $\beta = 1 - (1 - \frac{m}{H}) \times \tau$.

The proof of Corollary 2 can be found in Appendix C of the supplementary document. Accordingly, we should have a different upper and lower bounds for η as follows.

Corollary 3. *If all reference points are shifted onto the ROI, we can set $0 < \tau < 1$.*

The proof of Corollary 3 can be found in Appendix D of the supplementary document. Fig. 1(c) gives an example that all reference points have been shifted onto the ROI.

3.6 Algorithmic Details

After describing the mathematical foundations of the NUMS, this section describes its algorithmic implementation whose pseudo-code is presented in Algorithm 1. First of all, $N = \binom{H+m-1}{m-1}$ reference points $\mathbf{w}^1, \dots, \mathbf{w}^N$ are initialised via the Das and Dennis's method (line 1 of Algorithm 1). Afterwards, we find the pivot point (line 2 of Algorithm 1). Then, if the DM is interested in the boundary, we use Theorem 1 to compute the exponent η of the PDF in equation (2); otherwise, we use Corollary 2 to do so (line 3 to line 7 of Algorithm 1). During the main loop, for each reference point, we use equation (9) to determine the position of the corresponding boundary point for the non-uniform mapping (line 9 of Algorithm 1). If the currently investigating reference point lying on the boundary of Ψ^m and the DM is not interested in the boundary, we use equation (12) to determine the step-length for shifting this boundary reference point onto the ROI (line 11 of Algorithm 1); otherwise we use equation (5) and equation (7) to serve this purpose (line 13 and line 14 of Algorithm 1). At the end of this loop, we use equation (6) to calculate the new position of the biased reference point (line 15 of Algorithm 1).

3.7 Incorporation of the NUMS into a Decomposition-based EMO Algorithm

In principle, the NUMS can be readily incorporated into any decomposition-based EMO algorithm, e.g. MOEA/D and NSGA-III, in a plug-in manner. In particular, we only need to replace the reference points with the ones generated by the NUMS. However, for MOEA/D and its variants, the commonly used subproblem formulation, e.g. the Tchebycheff function, will only result in the population that are dominated by the ideal point [49], i.e. $\mathbf{z}^* = (z_1^*, \dots, z_m^*)^T$, where $z_i^* = \min_{\mathbf{x} \in PS} f_i(\mathbf{x})$ for all $i \in \{1, \dots, m\}$, which is unknown a priori. Although the ideal point can be estimated by the currently evolving population, it is highly likely that the estimated ideal point is away from the DM supplied aspiration level vector, as shown in Fig. 6. Note that it is fine if the DM wants to approximate the boundary and the ROI together, since the solutions on the boundary can give the appropriate ideal point. Otherwise, the algorithm will be struggling to obtain acceptable solutions if the DM is only interested in the ROI.

Algorithm 1: Non-uniform Mapping Scheme

Input:

- DM supplied aspiration level vector \mathbf{z}^r
- Number of divisions H
- Expected extent of ROI τ
- flag determines whether keep the boundary or not

Output:

- Biased reference points $\bar{W} \leftarrow \{\bar{\mathbf{w}}^1, \dots, \bar{\mathbf{w}}^N\}$

```

1 Initialize  $N \leftarrow \binom{H+m-1}{m-1}$  reference points  $\mathbf{w}^1, \dots, \mathbf{w}^N$  on a canonical simplex  $\Psi^m$  by Das and
  Dennis's method;
2 Find the pivot point  $\mathbf{w}^p$  of  $\mathbf{z}^r$  on  $\Psi^m$ ;
3 if flag = 1 then // keep the boundary
4    $\alpha \leftarrow \frac{m}{H}, \beta \leftarrow 1 - \tau$ ;
5 else
6    $\alpha \leftarrow \frac{m}{H}, \beta \leftarrow 1 - (1 - \frac{m}{H}) \times \tau$ ;
7  $\eta \leftarrow \frac{\log \alpha}{\log \beta} - 1$ ;
8 for  $i \leftarrow 1$  to  $N$  do
9    $\Delta \leftarrow \min_{1 \leq j \leq m} [w_j^p \times \frac{\|\mathbf{w}^p - \mathbf{w}^i\|}{w_j^p - w_j^i}]_+$ ;
10  if  $\Delta - \|\mathbf{w}^i - \mathbf{w}^p\| < \epsilon \wedge \text{flag} = 0$  then
11     $\rho \leftarrow \tau \times \|\mathbf{w}^i - \mathbf{w}^p\|$ ;
12  else
13     $\delta \leftarrow \Delta (\frac{\Delta - \ell}{\Delta})^{\frac{1}{\eta+1}}$ , where  $\ell \leftarrow \|\mathbf{w}^i - \mathbf{w}^p\|$ ;
14     $\rho \leftarrow \Delta - \delta$ ;
15   $\bar{\mathbf{w}}^i \leftarrow \mathbf{w}^p + \rho \times \frac{\mathbf{w}^i - \mathbf{w}^p}{\|\mathbf{w}^i - \mathbf{w}^p\|}$ ;
16 return  $\bar{W}$ 

```

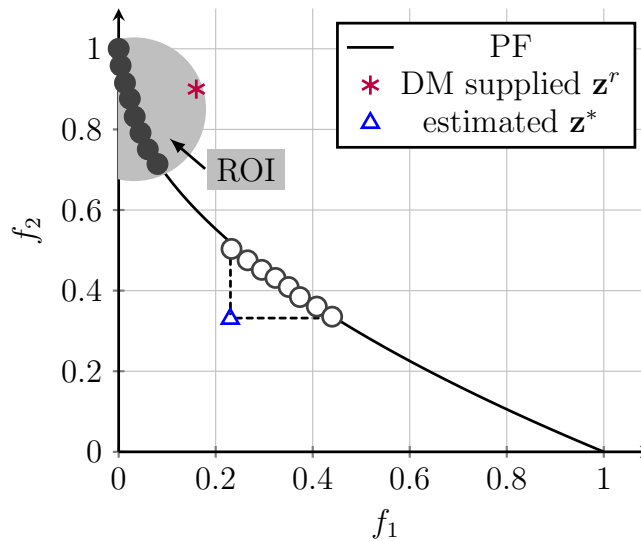


Figure 6: The estimated ideal point \mathbf{z}^* is away from the DM supplied aspiration level vector \mathbf{z}^r .

To overcome this aforementioned drawback, we use the following subproblem formation in MOEA/D and its variants:

$$\begin{aligned} \text{minimize} \quad & g(\mathbf{x}|\mathbf{w}, \mathbf{z}^r) = \max_{1 \leq i \leq m} \{w_i(f_i(\mathbf{x}) - z_i^r)\} \\ & + \rho \sum_{i=1}^m w_i(f_i(\mathbf{x}) - z_i^r) \quad , \\ \text{subject to} \quad & \mathbf{x} \in \Omega \end{aligned} \quad (14)$$

where Ω is the decision space and ρ is a sufficiently small positive number, which we set as 10^{-6} as suggested in [41]. As discussed in [50], the optimum of equation (14) must be a Pareto-optimal solution, and ρ is able to avoid the generation of weakly Pareto-optimal solutions. By using this subproblem formulation, we can expect that the search directions are heading toward the DM supplied aspiration level vector.

4 Proof-of-Principle Results

In this section, we empirically validate the effectiveness of the NUMS for assisting the decomposition-based EMO algorithms seek the DM's preferred solutions on problem instances with 2 to 10 objectives. Our recently proposed MOEA/D variant based on stable matching model, named MOEA/D-STM [51] is used as the baseline algorithm. Different from the canonical MOEA/D, where the selection of the next parents is merely determined by the aggregation function value of a solution, MOEA/D-STM treats subproblems and solutions as two sets of agents and considers their mutual preferences simultaneously. In particular, the preference of a subproblem over a solution measures the convergence issue, while the preference of a solution over a subproblem measures the diversity issue. Since the stable matching achieves an equilibrium of the mutual preferences between subproblems and solutions, MOEA/D-STM strikes a balance between convergence and diversity of the search process. Here we use the simulated binary crossover (SBX) [52] and the polynomial mutation [53] as the reproduction operators. For the SBX, the crossover probability is set as $p_c = 1.0$ and its distribution index is set as $\eta_c = 10$; for the polynomial mutation, the mutation probability is set as $p_m = \frac{1}{n}$ and its distribution index is set as $\eta_m = 20$. ZDT [54] and DTLZ [55] problem suites are chosen to form the benchmark.

Generally speaking, the proof-of-principle studies consist of two parts. First of all, we validate the effectiveness of the NUMS on the problem instances with two and three objectives. Afterwards, we empirically demonstrate some interesting extensions of the NUMS for handling various other scenarios, i.e. problems with many objectives, multiple ROIs and an interactive preference incorporation.

4.1 Problems with Two and Three Objectives

Let us start from the two-objective ZDT1 problem instance that has a convex PF [54]. The population size of MOEA/D-STM is set to 100 and it performs 300 generations. Fig. 7 shows a comparative results of solutions obtained by MOEA/D-STM with different τ settings. From this figure, we clearly see that the NUMS adapts the originally evenly distributed reference points to a biased distribution according to the required extent. In the meanwhile, MOEA/D-STM provides a well approximation of the partial PF with respect to those biased reference points. Note that, in order to approximate the whole PF without preference on any particular region, we need to set $\tau = 1 - \frac{2}{99}$ rather than 1.0 according to Theorem 1.

Next, we assess the performance of MOEA/D-STM with the NUMS on the three-objective DTLZ1 and DTLZ2 problem instances respectively. Here we set $\tau = 0.2$ in the NUMS, and MOEA/D-STM performs 300 generations for DTLZ2 and 1,000 generations for DTLZ1 due to its multi-modality. As shown in Fig. 8 and Fig. 9, with either an infeasible ($\mathbf{z}^r = (0.3, 0.3, 0.2)^T$ for DTLZ1) or feasible ($\mathbf{z}^r = (0.3, 0.5, 0.6)^T$ for DTLZ2) aspiration level vector, MOEA/D-STM has no difficulty in finding the preferred solutions in the ROI. Furthermore, MOEA/D-STM also well approximates the boundaries for both cases.

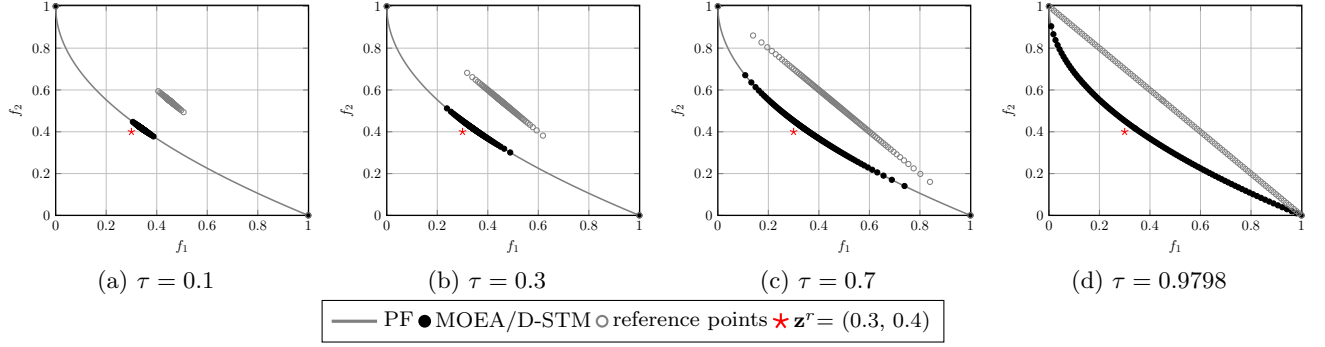


Figure 7: Comparisons of solutions obtained by MOEA/D-STM with different τ settings for NUMS on ZDT1 problem.

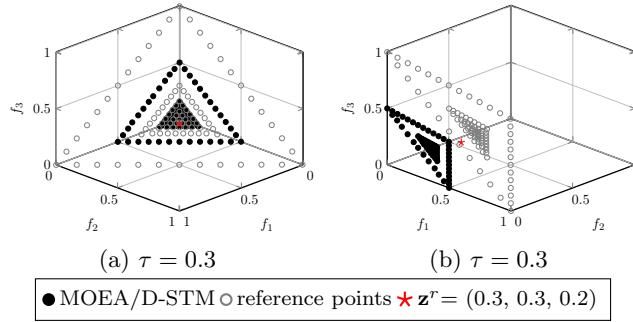


Figure 8: Solutions obtained by MOEA/D-STM on DTLZ1 problem where $\mathbf{z}^r = (0.3, 0.3, 0.2)^T$.

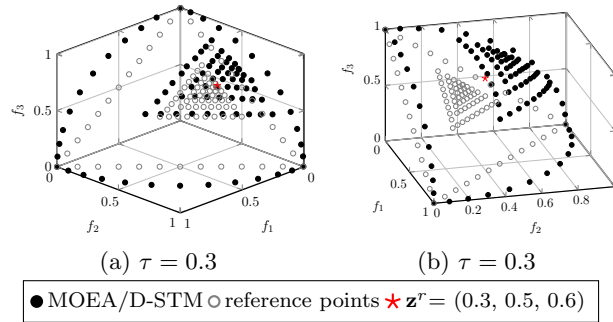


Figure 9: Solutions obtained by MOEA/D-STM on DTLZ2 problem where $\mathbf{z}^r = (0.2, 0.5, 0.6)^T$.

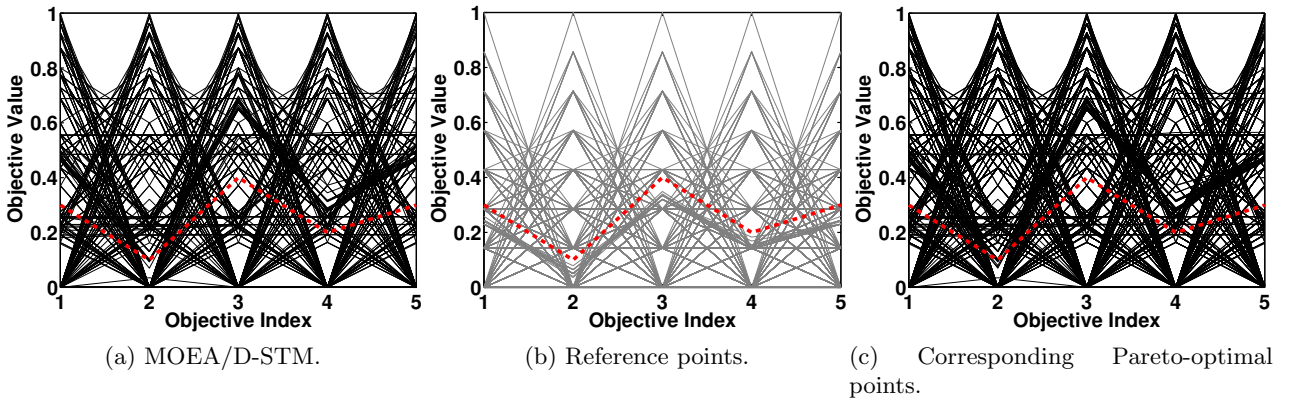


Figure 10: Solutions obtained by MOEA/D-STM on 5-objective DTLZ2 problem where $\mathbf{z}^r = (0.3, 0.1, 0.4, 0.2, 0.3)^T$ is represented as the red dotted line.

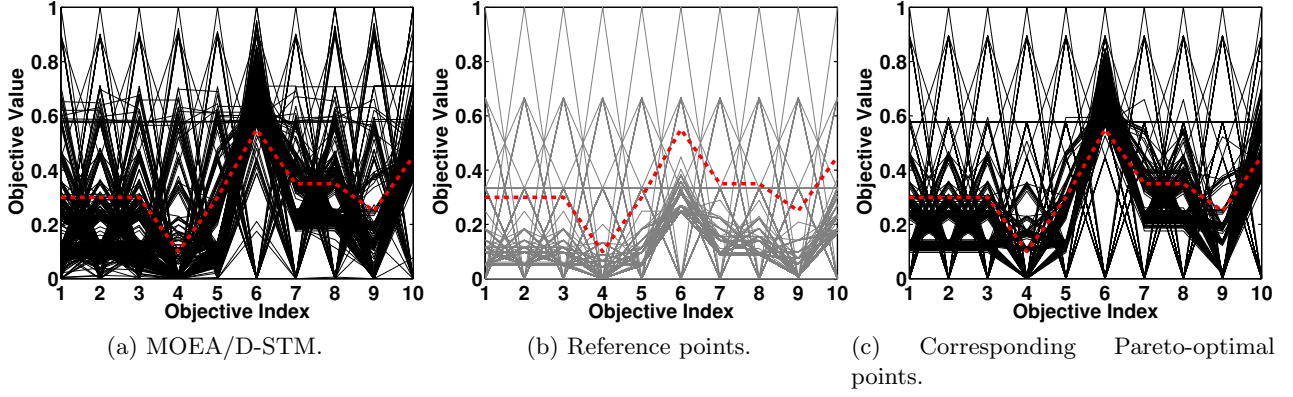


Figure 11: Solutions obtained by MOEA/D-STM on 10-objective DTLZ2 problem where $\mathbf{z}^r = (0.3, 0.3, 0.3, 0.1, 0.3, 0.55, 0.35, 0.35, 0.25, 0.45)^T$ is represented as the red dotted line.

4.2 Problems with Many Objectives

Now let us consider the five-objective DTLZ2 problem instance where $\mathbf{z}^r = (0.3, 0.1, 0.4, 0.2, 0.3)^T$. Now, we set $H = 7$ in the Das and Dennis's method which generates 330 uniformly distributed reference points, and τ is set to 0.1 in the NUMS. Fig. 10(c) gives the corresponding Pareto-optimal points, with respect to the biased reference points given in Fig. 10(b), according to the method developed in [56]. Comparing Fig. 10(a) with Fig. 10(c), we can see that MOEA/D-STM, after performing 1,000 generations, has a well approximation to both the ROI and the boundary points.

As discussed in [56] and [57], in order to have intermediate reference points within the simplex, we should set $H \geq m$ in the Das and Dennis's method. Otherwise, all reference points should lie on the boundary of the simplex. However, in a large-dimensional space, we can have a huge amount of reference points even when $H = m$. For example, when $m = 10$, the Das and Dennis's method can generate $\binom{10+10-1}{10-1} = 92378$ uniformly distributed reference points if $H = 10$. Obviously, current EMO algorithms cannot hold such huge number of solutions in a population. Even worse, when $H = m$, there is only one intermediate reference point which lies in the center of the simplex. Thus, the original NUMS might not be directly applicable when facing a large number of objectives. Inspired by the multi-layer weight vector generation method developed in [56] and [57], we make a slight modification to adapt the NUMS to the many-objective scenario. First of all, we use the Das and Dennis's method, where $H < m$, more than one time, to generate ($l > 1$) layers of reference points. Afterwards, we use the method developed in Section 3.5 to shift these reference points, which lie on the boundary of the simplex, onto the ROI layer by layer. Fig. 11(b) shows an example of 661 reference points generated by the multi-layer NUMS where $\mathbf{z}^r = (0.3, 0.3, 0.3, 0.1, 0.3, 0.55, 0.35, 0.35, 0.25, 0.45)^T$. In particular, we first use the Das and Dennis's method to generate $l = 3$ layers of reference points. Since we set $H = 3$, each layer contains 220 reference points. Then two layers of them are shifted onto the ROI, where the shrinkage factor τ is set to 0.4 and 0.2 respectively. Fig. 11(a) shows the final solutions obtained by MOEA/D-STM after 1,000 generations. Comparing to the corresponding Pareto-optimal points shown in Fig. 11(c), we can see that MOEA/D-STM still has a satisfactory approximation to the ROI in a 10-objective space.

4.3 Investigations on multiple ROIs

In practice, the DM might not be sure about his/her exact preferences and he/she would like to simultaneously explore several ROIs. In this case, the DM would like to supply more than one, say $T > 1$, aspiration level vectors at a time. To accommodate multiple ROIs, we only need to apply the NUMS T times with respect to each aspiration level vector. Note that each time the NUMS can preserve the boundary reference points, but we only need to keep these boundary reference points once. In other words, the duplicated boundary reference points are exempted from the final reference point set. Fig. 12 shows an example of two aspiration level vectors. In particular, the gray points are

the adapted reference points for each ROI; while the black points are the final solutions obtained by MOEA/D-STM with respect to the corresponding reference points. From the experimental results, we can clearly see that MOEA/D-STM with the NUMS is also able to approximate multiple ROIs simultaneously.

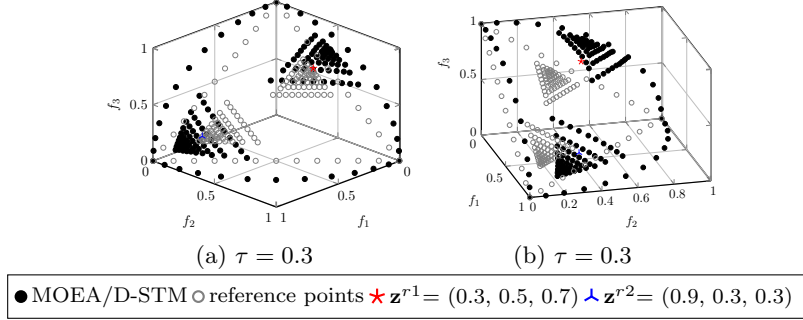


Figure 12: Solutions obtained by MOEA/D-STM with two different reference points on DTLZ2 problem.

4.4 Interactive Scenario

In practice, it is not uncommon that the DM is not fully confident about his/her elicited preference information due to the black box property of the problem itself. Therefore, an interactive decision-making procedure where the DM can progressively adapt his/her preference information during the optimisation process is attractive in the preference-based EMO. Since the NUMS can easily adapt the distribution of reference points to be biased toward the ROI, it facilitates the interactive scenario. Moreover, also due to the lack of the knowledge of the PF, the DM can easily specify an aspiration level vector which is beyond the boundary of the PF. Since the NUMS is able to preserve the boundary reference points, it finally helps the DM better understand the PF (e.g. its general shape, boundary, ideal and nadir points) and further adjusts his/her preference information. In Fig. 13, we describe an interactive run, which includes three cycles, of MOEA/D-STM on the DTLZ2 problem. We call a run of MOEA/D-STM for a certain number of generations specified by the DM as a cycle. First, as shown in Fig. 13(a), the DM specifies an aspiration level vector $\mathbf{z}_1^r = (1.4, 1.9, 1.5)^T$ beyond the PF. After 200 generations, MOEA/D-STM finds the solutions not only crowd in the ROI, but also distribute along the boundary. Thereafter, the DM realises that \mathbf{z}_1^r is a bad choice, and then he/she resets another aspiration level vector, say $\mathbf{z}_2^r = (0.7, 0.6, 0.3)^T$. In addition, since the DM already knows the boundary of the PF, he/she might not be interested in the boundary any longer. Thus, he/she sets the NUMS to adapt all reference points to the ROI. By using the final population of the first interaction as the initial population, MOEA/D-STM finally finds the solutions in the ROI after 200 generations. However, we assume that the DM still does not satisfy them and he/she sets another aspiration level vector, say $\mathbf{z}_3^r = (0.3, 0.4, 0.8)^T$. After 200 generations, as shown in Fig. 13(c), MOEA/D-STM finds the solutions in the vicinity of the ROI. This time, the DM is comfortable with the obtained solutions and this interactive EMO process terminates.

5 Comparisons with the State-of-the-Art

The proof-of-principle results shown in Section 4 fully demonstrated the effectiveness of the NUMS for assisting a decomposition-based EMO algorithm (here we use MOEA/D-STM as an example) search for preferred solutions in the ROI. As discussed in Section 2, there are some other preference-based EMO algorithms proposed in the EMO literature. In this section, we compare the performance of three state-of-the-art decomposition-based EMO algorithms, i.e. MOEA/D-STM, MOEA/D [6] and NSGA-III [16], assisted by the NUMS, where τ is set as 0.2, with three state-of-the-art preference-based EMO algorithms, i.e. g-NSGA-II [45], R-NSGA-II [12] and r-NSGA-II [13]. Note that different preference elicitation methods represent DM's distinct perspectives for comparing preferred solutions.

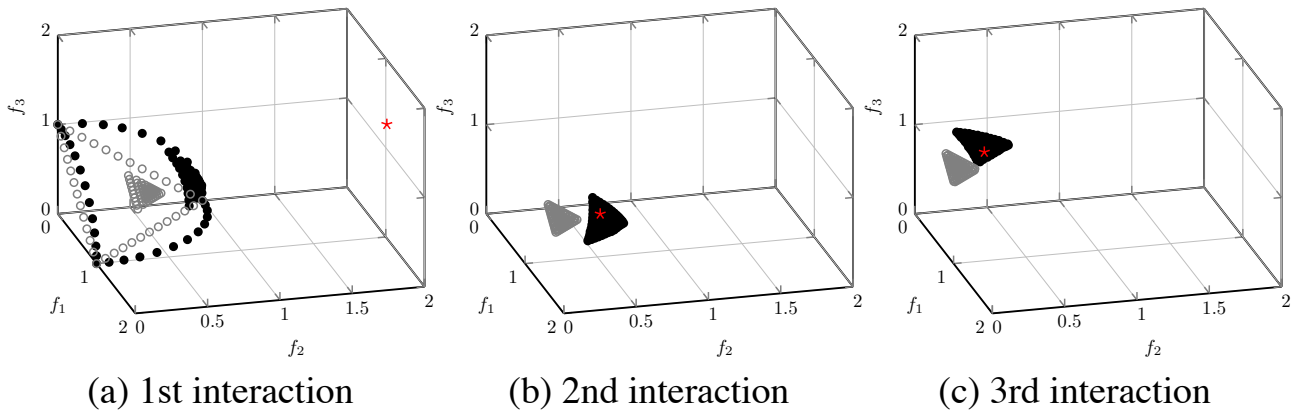


Figure 13: Interactive scenario on DTLZ2 problem.

For peer comparison purpose, here all these preference-based EMO algorithms use the aspiration level vector to elicit the DM’s preference information. All the multi-objective optimisers use the SBX and the polynomial mutation for offspring generation. The corresponding parameters are set the same as Section 4. In the experiments, we choose the popular DTLZ1 to DTLZ4, and WFG41 to WFG48 test problems [58] to form the benchmark suite. Note that WFG41 to WFG48 problems are designed to have various complex PF shapes, e.g. sharp convex/concave, mixed shape and disconnected PF segments. For DTLZ problems, $m \in \{3, 5, 8, 10\}$; while for WFG problems, $m \in \{2, 3, 5, 8, 10\}$. The settings of aspiration level vectors used in our experiments are given in Appendix E of the supplementary document. The population size is set as $N = 100$ when $m = 2$; $N = 92$ when $m = 3$; $N = 210$ when $m = 5$; $N = 360$ when $m = 8$; and $N = 660$ when $m = 10$, respectively. As for the NUMS, the number of divisions is set as $H = 13$ when $m = 3$ and $H = 6$ when $m = 5$. When the number of objectives is larger than 5, we use a 3-layer method suggested in Section 4.2 to generate the initially evenly distributed reference points. In particular, we set $H = 3$ for each layer. In our experiments, the stopping criterion of a preference-based EMO algorithm is the number of function evaluations (FEs), where the detailed settings are given in Appendix E of the supplementary document. As for R-NSGA-II, the additional parameter ϵ , used in its ϵ -clearing procedure, is set according to [12], i.e. $\epsilon = 0.001$ when $m = 2$ and $\epsilon = 0.01$ otherwise.

To quantitatively compare the performance of different preference-based EMO algorithms for approximating the ROI, we use our recently developed R-HV [59] and the Quality metric developed in [60, 61] as the performance indicators. In particular, the basic idea of R-HV computation is to pre-process the obtained preferred solution set S , according to the DM supplied \mathbf{z}^r , before using the hypervolume (HV) [62] for performance assessment. More interested readers can find the technical details of the R-HV computation in [59]. Similar to HV, the larger is the R-HV value, the better is the quality of S for approximating the ROI.

In the experiments, each algorithm is performed 31 independent runs. In the data tables, we show the median and the interquartile range (IQR) of metric values for different problem instances with various aspiration level vector settings. In particular, the best median metric values are highlighted in bold face with a grey background. To have a statistically sound conclusion, we carry out the statistical analysis as suggested in [63] to validate the statistical significance of the results. More detailed description of this statistical analysis framework is provided in Appendix F of the supplementary document. Here we only present the results on R-HV, while the data on Quality metric are put in Section H of the supplementary document. In addition, to have a visual comparison, we also show the scatter plots and the parallel coordinate plots (PCP), in the supplementary document, of the final solutions obtained by different algorithms having the best R-HV value.

5.1 Experimental Results

Due to the page limit, we only discuss the results on DTLZ problems, while the discussion on WFG problems can be found from Section G of the supplementary document. From the results shown

in Table 1, we can clearly see that the decomposition-based EMO algorithms, i.e. MOEA/D-STM, MOEA/D and NSGA-III, assisted by the NUMS are the best candidates for approximating the ROI of various test problems. Their superiority becomes more evident with the increase of the number of objectives. In the following paragraphs, we explain the results instance by instance.

Let us start from the DTLZ1 problem which has a linear PF shape, i.e. a hyper-plane intersects with each coordinate at 0.5. Note that DTLZ1 also has many local optima in its search space, which obstruct the convergence toward the global PF. In the 3-objective case, all algorithms, except g-NSGA-II, are able to drive solutions to converge toward the PF. As the DM expects the ROI to be 20% of the whole PF, solutions found by the decomposition-based EMO algorithms assisted by the NUMS are the best candidates with respect to the DM's expectation. Fig. 14 shows the scatter plots of solutions obtained by all algorithms with respect to $\mathbf{z}^r = (0.05, 0.05, 0.2)$. From this figure, we can see that solutions obtained by three decomposition-based EMO algorithms assisted by the NUMS are consistent and well distributed. In contrast, although the solutions found by R-NSGA-II are in the ROI, they crowd in a narrow region. In this case, R-NSGA-II cannot provide as many trade-off alternatives as the decomposition-based EMO algorithms assisted by the NUMS. As shown in Fig. 14, solutions found by r-NSGA-II do not converge to the ROI. With the increase of the number of objectives, g-NSGA-II and r-NSGA-II have difficulty in driving solutions toward the PF due to the multi-modal property of DTLZ1. As for R-NSGA-II, solutions are even more focused in the high-dimensional space as shown in Fig. 15, a 8-objective example with $\mathbf{z}^r = (0.01, 0.02, 0.07, 0.02, 0.06, 0.2, 0.1, 0.01)^T$. Although the spread of the preferred solutions obtained by R-NSGA-II can be controlled by its ϵ parameter, there is no rule-of-thumb for tuning it to adapt to the DM's expected extent of the ROI.

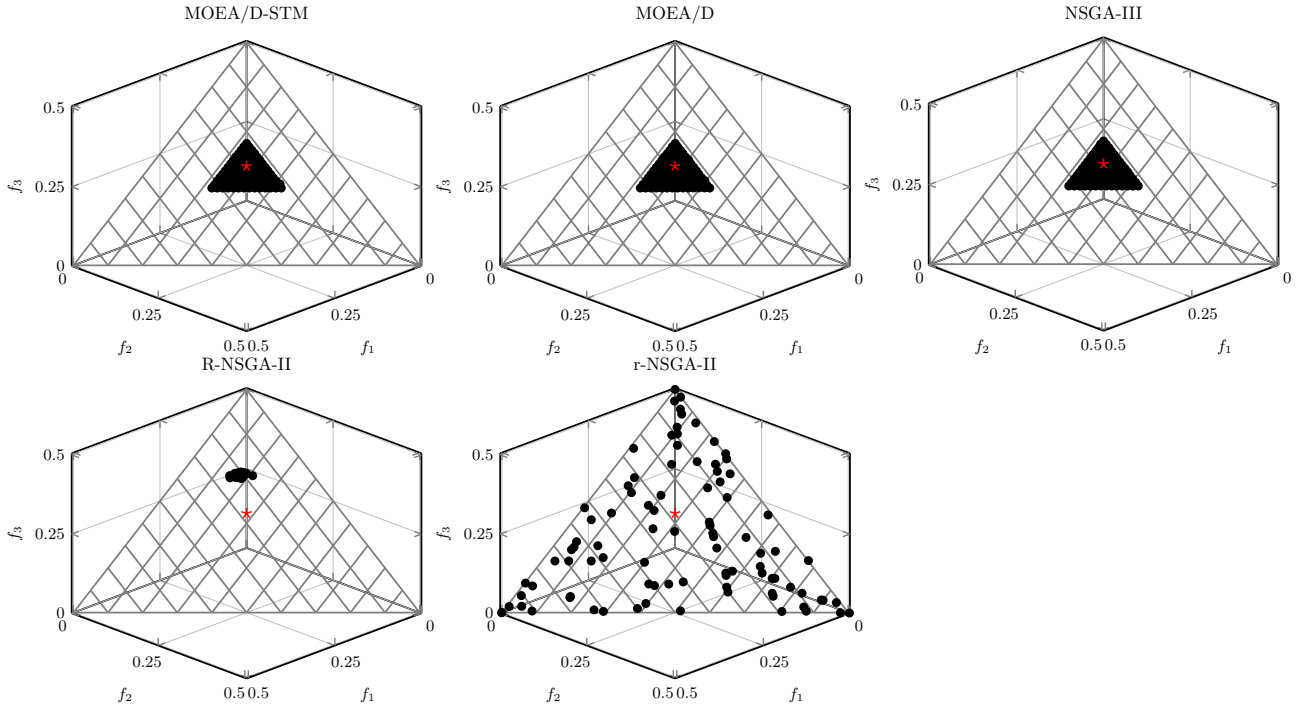


Figure 14: Scatter plots of solutions on 3-objective DTLZ1 where $\mathbf{z}^r = (0.05, 0.05, 0.2)$.

DTLZ2 is a relatively simple test problem, where the objective functions of a Pareto-optimal solution \mathbf{x}^* satisfies: $\sum_{i=1}^m f_i^2(\mathbf{x}^*) = 1$. All algorithms do not have too much difficulty in driving solutions toward the PF. As the examples shown in Fig. 16 and Fig. 17, the performance of three decomposition-based EMO algorithms assisted by the NUMS are consistent. In contrast, the spread of the solutions obtained by the other three preference-based EMO algorithms is not fully controllable. In particular, solutions found R-NSGA-II and r-NSGA-II are very focused while those found by g-NSGA-II scattered in a wide region.

The PF of DTLZ3 is the same as DTLZ2. But its search space contains many local optima which can make an EMO algorithm get stuck at any local PF before converging to the global PF. Similar to the observations in DTLZ1, g-NSGA-II cannot find any converged solutions in all 3- to 10-objective

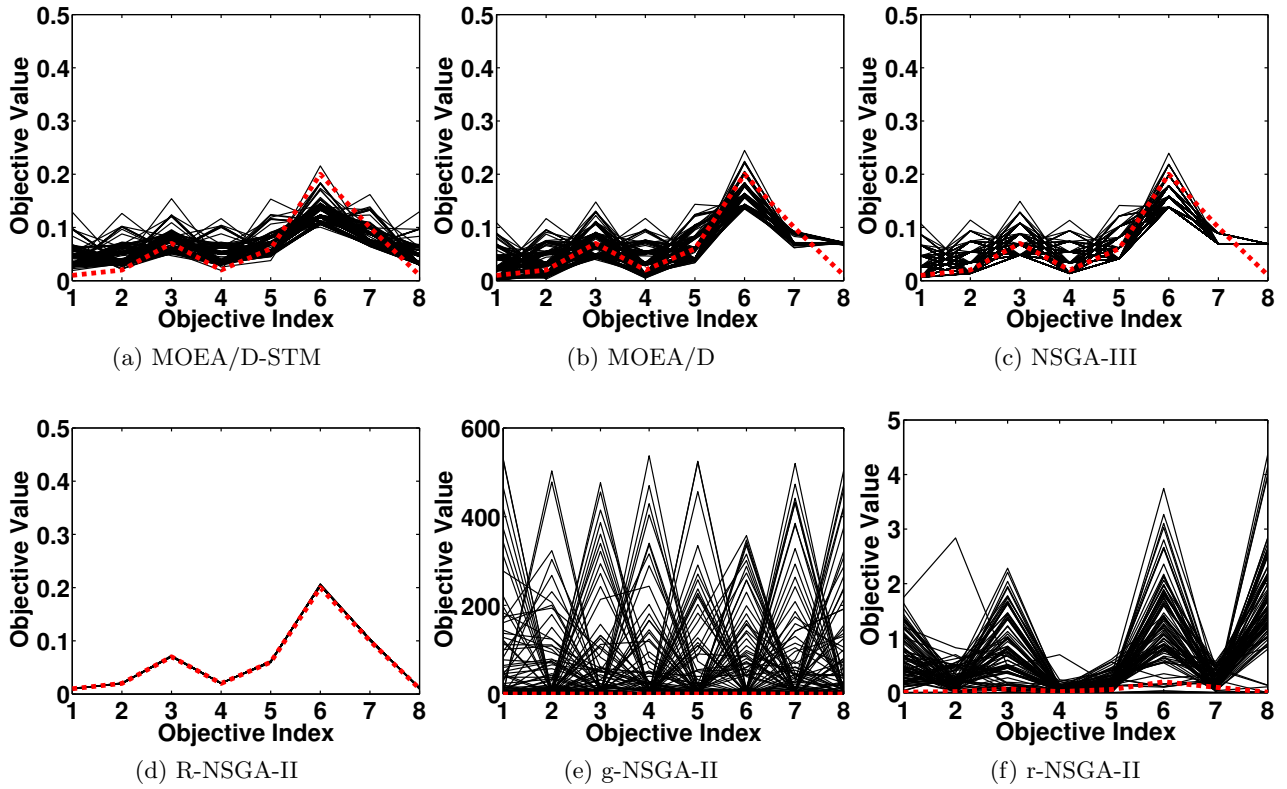


Figure 15: PCP of solutions on 8-objective DTLZ1 where $\mathbf{z}^r = (0.01, 0.02, 0.07, 0.02, 0.06, 0.2, 0.1, 0.01)^T$.

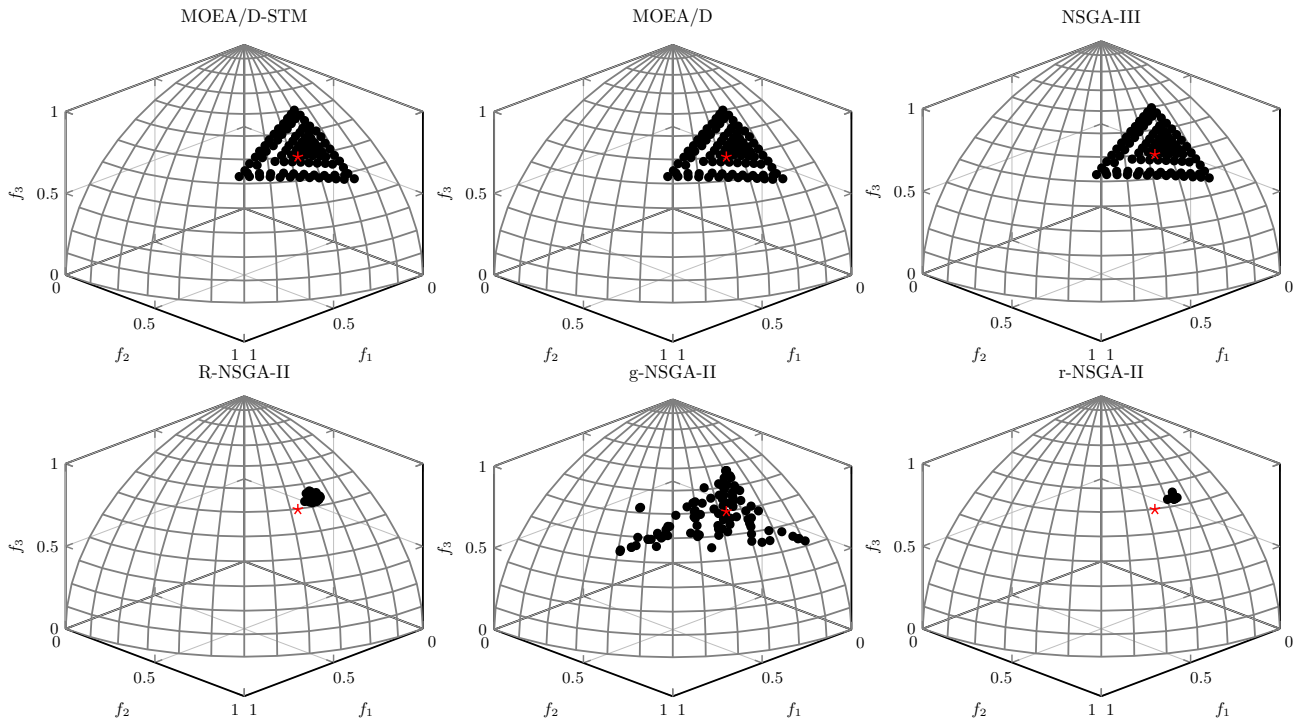


Figure 16: Scatter plots of solutions on 3-objective DTLZ2 where $\mathbf{z}^r = (0.2, 0.5, 0.6)$.

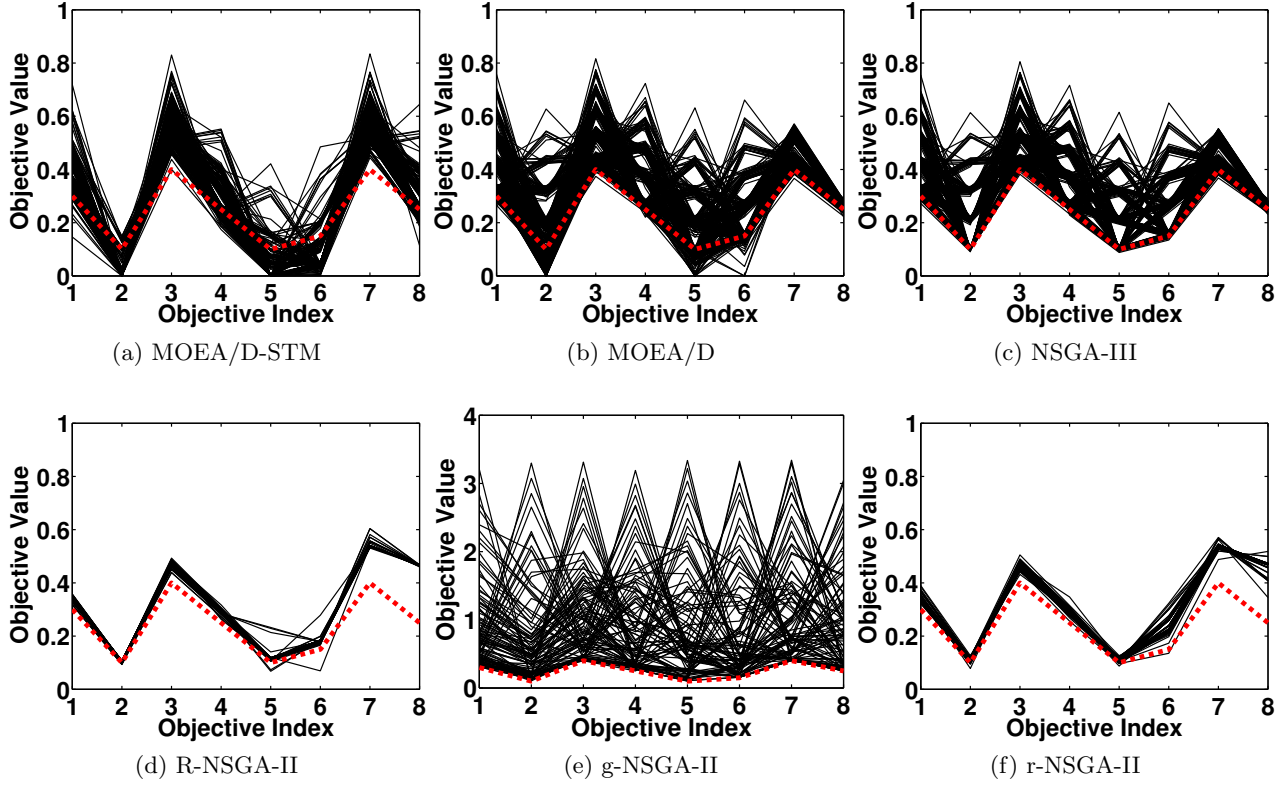


Figure 17: PCP of solutions on 8-objective DTLZ2 where $\mathbf{z}^r = (0.3, 0.1, 0.4, 0.25, 0.1, 0.15, 0.4, 0.25)^T$.

cases. The performance of the decomposition-based EMO algorithms assisted by the NUMS is very robust. It is interesting to note that, as the example shown in Fig. 18, solutions found by r-NSGA-II do not converge well to the ROI in the 3-objective case. This might be caused by the failure of its adaptive parameter control given a limited number of FEs. As shown in Fig. 19, we also notice that solutions found by r-NSGA-II do not converge to the PF when the number of objectives becomes large.

DTLZ4 also has the identical PF shape as DTLZ2. However, in order to investigate an EMO algorithm's ability to maintain a good distribution of solutions, DTLZ4 introduces a parametric variable mapping to the objective functions of DTLZ2. This modification allows a biased density of points away from $f_m(\mathbf{x}) = 0$. It is interesting to note that the performance of all these algorithms are similar to the DTLZ2. As the examples shown in Fig. 20 and Fig. 21, g-NSGA-II cannot drive all solutions converge to the PF due to the biased density of solutions. As shown in Fig. 20, some solutions found by r-NSGA-II are still drifted away from the PF when encountering an attainable aspiration level vector, i.e. $\mathbf{z}^r = (0.7, 0.8, 0.5)$, in the 3-objective case.

5.2 Summary of the Experimental Results

Based on the observations in Section 5.1, we summarise the comparisons between the decomposition-based EMO algorithms assisted by the NUMS and the other preference-based EMO algorithms as follows.

- Solutions found by three decomposition-based EMO algorithms assisted by the NUMS are consistent. This is because the search directions of a decomposition-based EMO algorithm is determined by the reference points. By using the NUMS, the reference points are transformed from an even distribution to a biased distribution toward the DM supplied aspiration level vector. In contrast, the driving force of the other preference-based EMO algorithms is to find solutions close to the DM supplied aspiration level vector. Since this 'closeness' by itself is vague, it brings uncertainty to the search process.

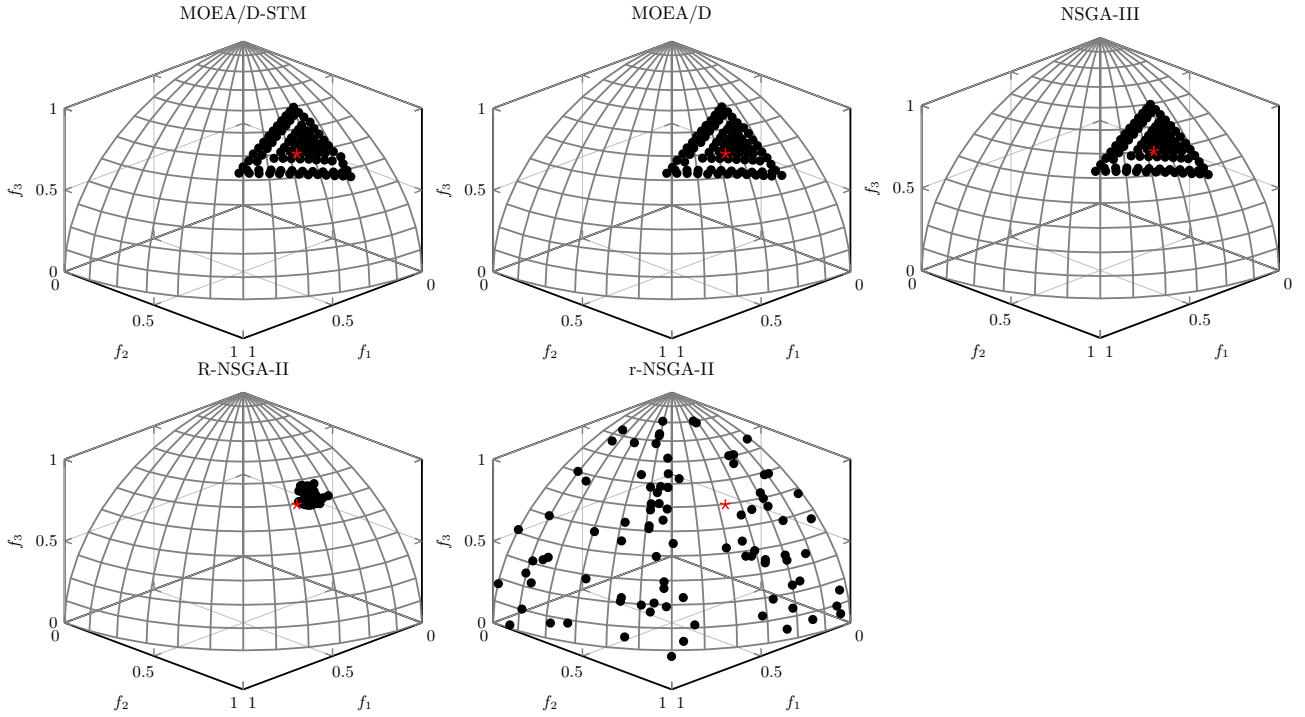


Figure 18: Scatter plots of solutions on 3-objective DTLZ3 where $\mathbf{z}^r = (0.2, 0.5, 0.6)$.

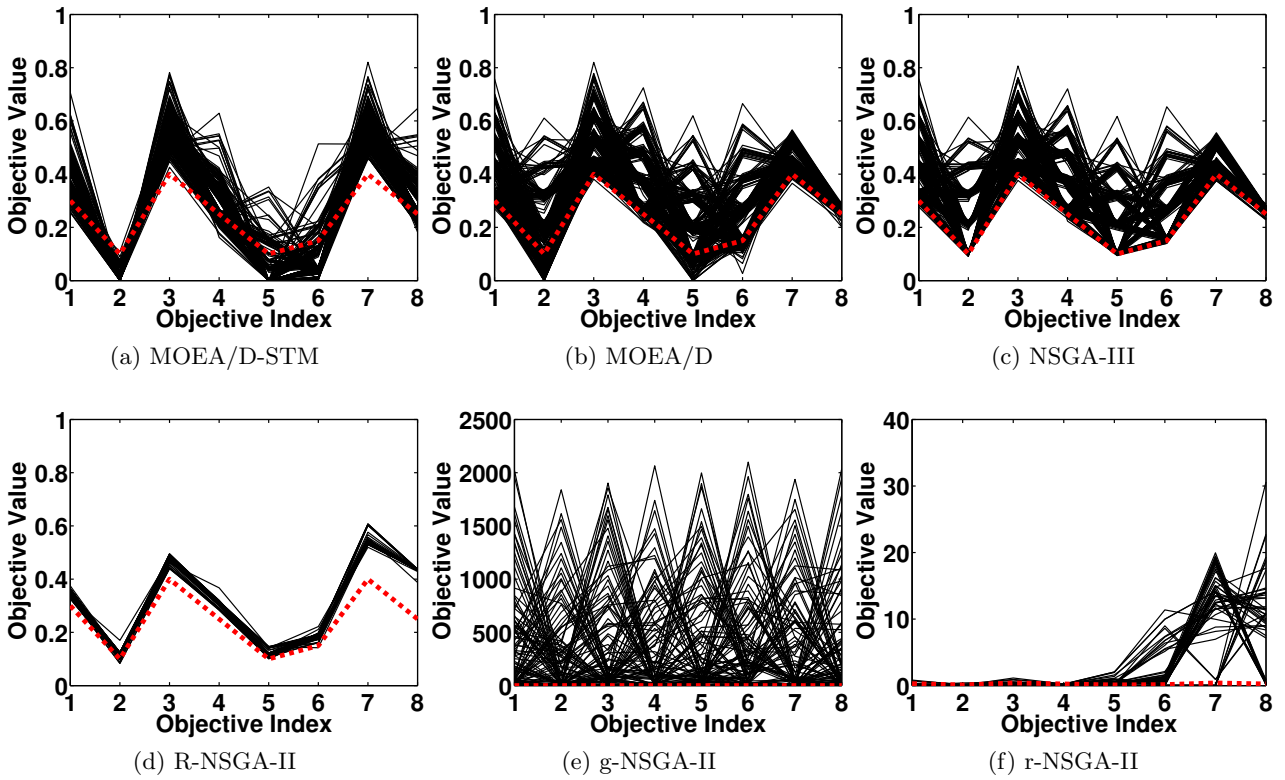


Figure 19: PCP of solutions on 8-objective DTLZ3 where $\mathbf{z}^r = (0.3, 0.1, 0.4, 0.25, 0.1, 0.15, 0.4, 0.25)^T$.

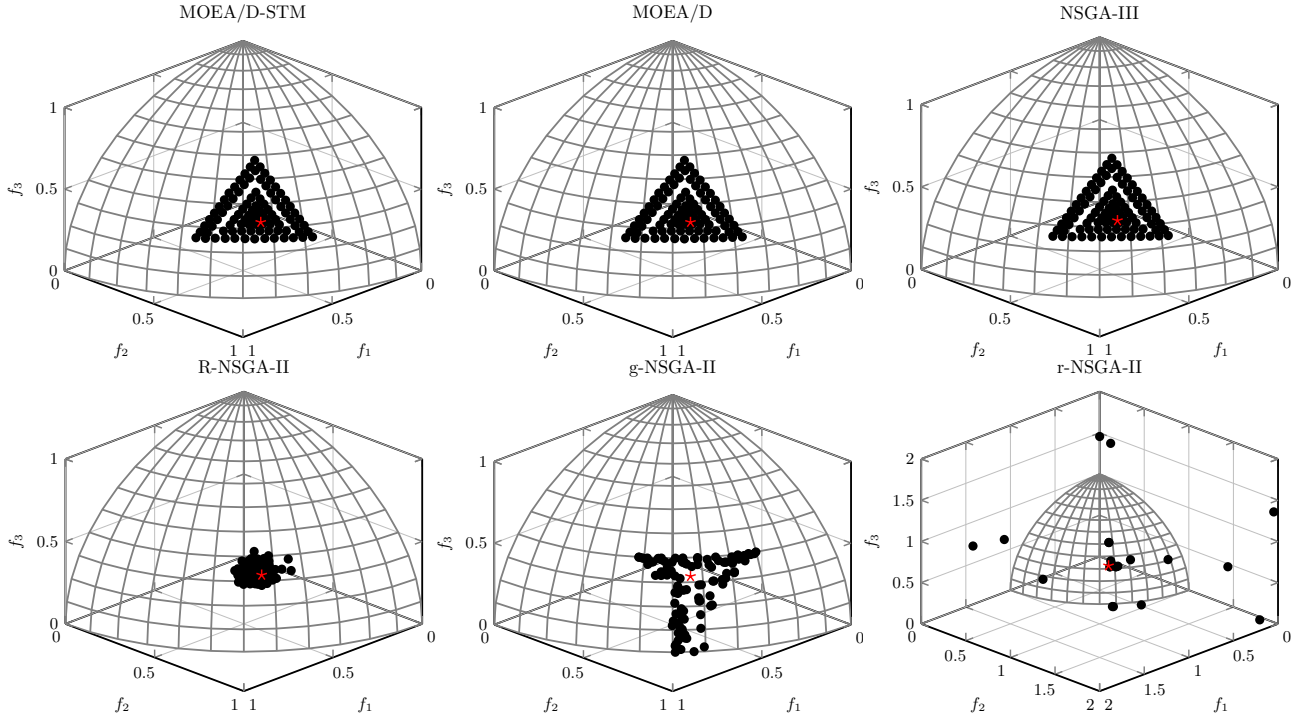


Figure 20: Scatter plots of solutions on 3-objective DTLZ4 where $\mathbf{z}^r = (0.7, 0.8, 0.5)$.

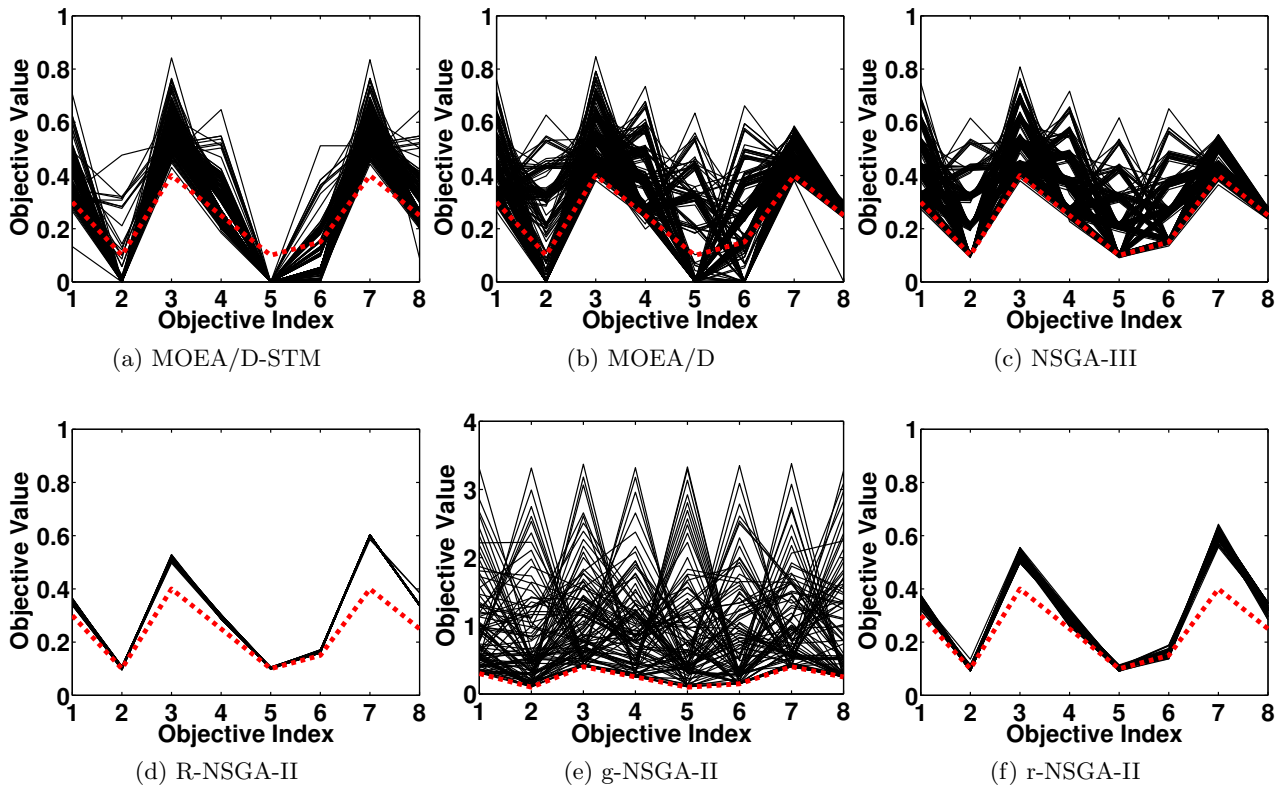


Figure 21: PCP of solutions on 8-objective DTLZ4 where $\mathbf{z}^r = (0.3, 0.1, 0.4, 0.25, 0.1, 0.15, 0.4, 0.25)^T$.

Table 1: Comparison results of median R-HV values and the IQR obtained by six preference-based EMO algorithms on DTLZ1 to DTLZ4 problems with unattainable and attainable aspiration level vectors.

Problem	m	ref	MOEA/D-STM	MOEA/D	NSGA-III	g-NSGA-II	r-NSGA-II	R-NSGA-II
DTLZ1	3	1	7.6265(1.36E-2)	7.5576(4.02E-3) [†]	7.5421(7.44E-1) [†]	–	7.5020(4.20E-1) [†]	7.0634(3.52E-1) [†]
		2	9.7153(5.05E-3)	9.6196(4.59E-3) [†]	9.5774(1.32E-1) [†]	–	9.4421(5.32E-1) [†]	9.5067(2.42E-1) [†]
	5	1	30.3722(3.28E-2)	29.6851(6.83E-2) [†]	30.3514(2.29E-3) [†]	0.0(0.0) [†]	0.0(0.0) [†]	27.5884(1.83E+0) [†]
		2	39.9092(1.90E-1)	39.5070(8.40E-2) [†]	39.2911(2.01E-2) [†]	0.0(0.0) [†]	0.0(0.0) [†]	31.0169(8.04E-1) [†]
	8	1	256.1972(1.49E+0)	219.2751(2.12E+0) [†]	212.5726(9.78E-2) [†]	–	0.3206(6.57E+0) [†]	253.8647(1.58E+0) [†]
		2	394.1900(2.21E+0)	373.3217(1.18E+0) [†]	363.1069(8.42E-2) [†]	–	0.8242(3.31E+1) [†]	168.8741(3.10E+0) [†]
	10	1	983.9530(5.09E+0)	967.8723(4.19E+0) [†]	971.8743(6.21E+0) [†]	–	0.0(0.0) [†]	767.3413(3.36E+1) [†]
		2	1206.1236(3.38E+1)	1184.5294(4.23E+1) [†]	1169.5398(1.42E+1) [†]	0.0(0.0) [†]	0.0(0.0) [†]	853.7466(3.46E+1) [†]
DTLZ2	3	1	7.5535(9.37E-3) [†]	7.5907(2.73E-2) [†]	7.6154(3.08E-2)	7.4123(2.20E-1) [†]	6.6851(2.43E-1) [†]	6.9901(1.34E-1) [†]
		2	10.3925(3.72E-3)	10.3853(2.98E-2) [†]	10.3847(1.13E-2) [†]	10.3409(1.60E-1) [†]	7.8869(1.86E+0) [†]	9.8209(2.17E-1) [†]
	5	1	23.9962(1.66E-1)	21.3977(1.44E-1) [†]	22.4874(3.82E-2) [†]	0.1010(1.67E-1) [†]	17.0738(4.30E+0) [†]	18.5786(2.29E+0) [†]
		2	54.1961(3.16E+0)	49.8608(3.77E-1) [†]	49.4824(7.20E-2) [†]	0.9246(8.99E-1) [†]	20.8631(1.83E+0) [†]	20.0445(3.14E+0) [†]
	8	1	156.3257(3.81E+0) [†]	169.0146(1.87E+1)	155.7312(9.33E-1) [†]	0.0(0.0) [†]	148.6432(3.71E+1) [†]	128.4391(4.14E+1) [†]
		2	537.7850(1.02E+1)	467.3111(4.67E+1) [†]	383.7051(1.12E+0) [†]	0.0002(6.75E-3) [†]	225.2263(2.88E+1) [†]	200.2079(2.14E+1) [†]
	10	1	681.1106(9.34E+0)	613.2450(2.81E+1) [†]	618.5795(1.07E+1) [†]	0.0(0.0) [†]	583.1804(2.24E+2) [†]	552.1471(1.24E+2) [†]
		2	824.7383(1.36E+1) [†]	810.1624(2.52E+1) [†]	836.2942(1.52E+1)	–	253.0452(8.23E+1) [†]	–
DTLZ3	3	1	7.4957(3.17E-2) [†]	7.6179(1.58E-2)	6.4873(1.44E+0) [†]	–	6.8314(5.23E-1) [†]	7.0110(2.26E-1) [†]
		2	10.3562(1.15E-1) [†]	10.3889(1.48E-2)	9.1242(7.05E-1) [†]	–	9.2263(5.18E-1) [†]	9.4979(2.59E-1) [†]
	5	1	23.9185(1.88E-1)	21.3864(9.77E-1) [†]	22.4379(6.41E-2) [†]	0.0(0.0) [†]	0.0(0.0) [†]	19.4719(1.70E+0) [†]
		2	54.1003(3.19E+0)	50.3797(5.03E-1) [†]	49.5082(1.33E-1) [†]	0.0(0.0) [†]	0.0(0.0) [†]	19.3515(1.85E+0) [†]
	8	1	156.2452(5.22E+0) [†]	168.2266(1.60E+1)	155.0874(1.06E+0) [†]	–	0.0(0.0) [†]	142.7653(2.32E+1) [†]
		2	539.3116(1.13E+1)	485.6386(3.74E+1) [†]	383.3493(5.65E+0) [†]	–	0.0(0.0) [†]	209.8244(2.91E+1) [†]
	10	1	669.1227(2.52E+1)	619.1556(1.23E+1) [†]	616.6172(9.07E+0) [†]	–	0.0(0.0) [†]	598.6863(1.14E+2) [†]
		2	819.9696(1.43E+1)	816.5128(3.77E+1) [†]	818.4483(1.35E+1) [†]	–	0.0(0.0) [†]	–
DTLZ4	3	1	7.5538(6.98E-3) [†]	7.6164(8.44E-3)	5.5442(2.11E+0) [†]	7.4036(1.70E-1) [†]	6.8757(7.78E-2) [†]	7.2718(7.86E-2) [†]
		2	10.3923(6.16E-3)	10.3728(1.63E-1) [†]	9.2591(2.99E+0) [†]	10.2584(2.26E-1) [†]	7.0280(2.53E+0) [†]	10.1231(1.71E-1) [†]
	5	1	23.9222(3.20E-1)	21.3998(7.09E-3) [†]	22.4862(1.27E-2) [†]	3.9178(4.67E+0) [†]	18.6539(9.58E-1) [†]	16.6939(1.14E+0) [†]
		2	50.8973(1.80E+0)	50.1681(5.02E-1) [†]	49.4684(3.70E-2) [†]	11.2802(1.21E+1)	16.1376(2.14E+0) [†]	15.3083(3.37E+0) [†]
	8	1	155.8001(3.43E-1) [†]	181.2326(6.42E+0)	155.9706(6.61E-1) [†]	0.0(0.0) [†]	144.1317(2.12E+1) [†]	119.5649(7.86E+0) [†]
		2	540.3963(5.04E+0) [†]	541.2044(4.52E+1)	383.6760(2.45E+0) [†]	0.0(1.23E-2) [†]	220.2359(2.00E+1) [†]	190.5484(7.55E+0) [†]
	10	1	679.4695(1.21E+1)	603.9090(2.12E+1) [†]	621.5302(7.06E+0) [†]	0.0(0.0) [†]	636.6269(1.15E+2) [†]	421.0407(2.92E+1) [†]
		2	828.9138(1.14E+1) [†]	774.1783(3.92E+1) [†]	843.7055(4.30E+0)	–	187.1426(7.42E+1) [†]	–

[†] denotes the best median metric value is significantly better than the other peers according to the statistical analysis described in Appendix F of the supplementary document. ref = 1 means the unattainable aspiration level vector while ref = 2 means the attainable aspiration level vector. – means all solutions obtained by the corresponding algorithm are dominated by the other counterparts, thus no solution can be used for R-HV computation.

- For the decomposition-based EMO algorithms assisted by the NUMS, the extent of the approximated ROI is controlled by the DM in an intuitively understandable manner. For the other preference-based EMO algorithms, the approximated ROI can be any crowd of solutions ‘close’ to the DM supplied aspiration level vector. Although there are some parameters that control this extent, there is no rule-of-thumb to tweak those parameters.
- As shown in Section 4, the NUMS can help a decomposition-based EMO algorithm not only find solutions in the ROI, but also those lying on the boundary of the PF. In contrast, The other preference-based EMO algorithms can only approximate the ROI.
- Different from the other preference-based EMO algorithms, the NUMS does not incur additional computations to the baseline algorithm. As introduced in Section 3.7, we only need to change the distribution of the reference points to be biased toward the ROI. As shown in Table VIII of the supplementary document, the average CPU time costs of the NUMS assisted algorithms are almost the same as the baseline algorithms.

6 Conclusions

This paper present a systematic way to incorporate the DM’s preference information into the decomposition-based EMO methods in either a priori or interactive manner. In particular, the DM’s preference information is modelled as an aspiration level vector which represents the DM’s expected value on each objective. Our basic idea is a non-uniform mapping scheme that transforms the originally evenly distributed reference points into a biased distribution. In particular, the closer to the DM specified aspiration level vector, the more reference points in view of their higher relevance to the DM’s preference information. Different from the existing literature, the ROI’s size is fully controllable and intuitively understandable according to a quantitative definition. To facilitate the interactive decision-making process, our proposed NUMS is able to preserve the ones located on the boundary as well, given the DM’s requirements. By incorporating the NUMS into some decomposition-based EMO algorithms, i.e., MOEA/D-STM, MOEA/D and NSGA-III, its effectiveness is validated by proof-of-principle experiments and comparative studies with other state-of-the-art preference-based EMO algorithms on a variety of benchmark problems with 2 to 10 objectives.

It is clear that the distribution of the biased reference points is determined by the transformation function defined in equation (2). One direct extension of this paper is to use some other distribution functions that are tailored according to the DM’s requirements. As discussed in Section 2, there are several other ways of eliciting the DM’s preference information. The other extension of this work is the adaptation of the NUMS to other types of preference model. To further facilitate the interactive process, it is worth considering the combination of human computer interaction techniques [64] and the preference-based EMO. Moreover, discrete and mixed variable optimisation problems are ubiquitous in real-world applications, e.g. scheduling [60, 61]. It is interesting to study the application of the NUMS for finding DM preferred solutions in those cases.

Acknowledgment

This work was supported by the Ministry of Science and Technology of China (Grant No. 2017YFC0804003), the Royal Society (Grant No. IEC/NSFC/170243), the Science and Technology Innovation Committee Foundation of Shenzhen (Grant Nos. ZDSYS201703031748284), Shenzhen Peacock Plan (Grant No. KQTD2016112514355531), and EPSRC (Grant Nos EP/J017515/1 and EP/P005578/1).

References

- [1] K. Deb, A. Pratap, S. Agarwal, and T. Meyarivan, “A fast and elitist multiobjective genetic algorithm: NSGA-II,” *IEEE Trans. Evolutionary Computation*, vol. 6, no. 2, pp. 182–197, Apr. 2002.

- [2] A. E. I. Brownlee and J. A. Wright, “Constrained, mixed-integer and multi-objective optimisation of building designs by NSGA-II with fitness approximation,” *Appl. Soft Comput.*, vol. 33, pp. 114–126, 2015.
- [3] S. H. R. Pasandideh, S. T. A. Niaki, and K. Asadi, “Bi-objective optimization of a multi-product multi-period three-echelon supply chain problem under uncertain environments: NSGA-II and NREGA,” *Inf. Sci.*, vol. 292, pp. 57–74, 2015.
- [4] M. Rabiee, M. Zandieh, and P. Ramezani, “Bi-objective partial flexible job shop scheduling problem: NSGA-II, NREGA, MOGA and PAES approaches,” *International Journal of Production Research*, vol. 50, no. 24, pp. 7327–7342, 2012.
- [5] E. Zitzler and S. Künzli, “Indicator-based selection in multiobjective search,” in *PPSN’04: Proc. of the 8th International Conference on Parallel Problem Solving from Nature*, 2004, pp. 832–842.
- [6] Q. Zhang and H. Li, “MOEA/D: A multiobjective evolutionary algorithm based on decomposition,” *IEEE Trans. Evolutionary Computation*, vol. 11, pp. 712–731, Dec. 2007.
- [7] T. L. Saaty, “The modern science of multicriteria decision making and its practical applications: The ahp/analytic approach,” *Operational Research*, vol. 61, no. 5, pp. 1101–1118, 2013.
- [8] C. A. C. Coello, “Handling preference in evolution multiobjective optimization: A survey,” in *CEC’00: Proc. of the 2000 IEEE International Conference on Evolutionary Computation*, 2000, pp. 30–37.
- [9] L. Rachmawati and D. Srinivasan, “Preference incorporation in multi-objective evolutionary algorithms: A survey,” in *CEC’06: Proc. of the 2006 IEEE International Conference on Evolutionary Computation*, 2006, pp. 962–968.
- [10] R. C. Purshouse, K. Deb, M. M. Mansor, S. Mostaghim, and R. Wang, “A review of hybrid evolutionary multiple criteria decision making methods,” in *CEC’14: Proc. of the 2014 IEEE Congress on Evolutionary Computation*, 2014, pp. 1147–1154.
- [11] S. Bechikh, M. Kessentini, L. B. Said, and K. Ghédira, “Preference incorporation in evolutionary multiobjective optimization: A survey of the state-of-the-art,” in *Advances in Computers*, 2015, vol. 98, pp. 141–207.
- [12] K. Deb, J. Sundar, U. Bhaskara, and S. Chaudhuri, “Reference point based multiobjective optimization using evolutionary algorithms,” *International Journal of Computational Intelligence Research*, vol. 2, no. 3, pp. 273–286, 2006.
- [13] L. B. Said, S. Bechikh, and K. Ghédira, “The r-dominance: A new dominance relation for interactive evolutionary multicriteria decision making,” *IEEE Trans. Evolutionary Computation*, vol. 14, no. 5, pp. 801–818, 2010.
- [14] L. Thiele, K. Miettinen, P. J. Korhonen, and J. M. Luque, “A preference-based evolutionary algorithm for multi-objective optimization,” *Evolutionary Computation*, vol. 17, no. 3, pp. 411–436, 2009.
- [15] M. Köksalan and I. Karahan, “An interactive territory defining evolutionary algorithm: iTDEA,” *IEEE Trans. Evolutionary Computation*, vol. 14, no. 5, pp. 702–722, 2010.
- [16] K. Deb and H. Jain, “An evolutionary many-objective optimization algorithm using reference-point-based nondominated sorting approach, part I: solving problems with box constraints,” *IEEE Trans. Evolutionary Computation*, vol. 18, no. 4, pp. 577–601, 2014.
- [17] I. Das and J. E. Dennis, “Normal-Boundary Intersection: A new method for generating the pareto surface in nonlinear multicriteria optimization problems,” *SIAM Journal on Optimization*, vol. 8, pp. 631–657, 1998.

- [18] Y. Tan, Y. Jiao, H. Li, and X. Wang, “A modification to MOEA/D-DE for multiobjective optimization problems with complicated pareto sets,” *Information Sciences*, vol. 213, pp. 14–38, 2012.
- [19] S. Jiang, Z. Cai, J. Zhang, and Y. Ong, “Multiobjective optimization by decomposition with Pareto-adaptive weight vectors,” in *ICNC’11: Proc. of the 7th International Conference on Natural Computation*, 2011, pp. 1260–1264.
- [20] Y. Qi, X. Ma, F. Liu, L. Jiao, J. Sun, and J. Wu, “MOEA/D with adaptive weight adjustment,” *Evolutionary Computation*, vol. 22, no. 2, pp. 231–264, 2014.
- [21] I. Giagkiozis and P. J. Fleming, “Pareto front estimation for decision making,” *Evolutionary Computation*, vol. 22, no. 4, pp. 651–678, 2014.
- [22] X. Ma, F. Liu, Y. Qi, L. Li, L. Jiao, X. Deng, X. Wang, B. Dong, Z. Hou, Y. Zhang, and J. Wu, “MOEA/D with biased weight adjustment inspired by user preference and its application on multi-objective reservoir flood control problem,” *Soft Computing*, 2015, accepted for publication.
- [23] R. Cheng, Y. Jin, M. Olhofer, and B. Sendhoff, “A reference vector guided evolutionary algorithm for many-objective optimization,” *IEEE Trans. Evolutionary Computation*, 2016, accepted for publication.
- [24] K. Deb, “Multi-objective evolutionary algorithms: Introducing bias among pareto-optimal solutions,” in *Advances in Evolutionary Computing*, A. Ghosh and S. Tsutsui, Eds. Springer Berlin Heidelberg, 2003, pp. 263–292.
- [25] J. Branke and K. Deb, “Integrating user preferences into evolutionary multi-objective optimization,” in *Knowledge Incorporation in Evolutionary Computation*, Y. Jin, Ed. Springer Berlin Heidelberg, 2005, vol. 167, pp. 461–477.
- [26] S. P. Phelps and M. Köksalan, “An interactive evolutionary metaheuristic for multiobjective combinatorial optimization,” *Management Science*, vol. 49, no. 12, pp. 1726–1738, 2003.
- [27] J. W. Fowler, E. S. Gel, M. Köksalan, P. J. Korhonen, J. L. Marquis, and J. Wallenius, “Interactive evolutionary multi-objective optimization for quasi-concave preference functions,” *European Journal of Operational Research*, vol. 206, no. 2, pp. 417–425, 2010.
- [28] K. Deb, A. Sinha, P. J. Korhonen, and J. Wallenius, “An interactive evolutionary multiobjective optimization method based on progressively approximated value functions,” *IEEE Trans. Evolutionary Computation*, vol. 14, no. 5, pp. 723–739, 2010.
- [29] R. Battiti and A. Passerini, “Brain-computer evolutionary multiobjective optimization: A genetic algorithm adapting to the decision maker,” *IEEE Trans. Evolutionary Computation*, vol. 14, no. 5, pp. 671–687, 2010.
- [30] J. Branke, S. Greco, R. Slowinski, and P. Zielniewicz, “Learning value functions in interactive evolutionary multiobjective optimization,” *IEEE Trans. Evolutionary Computation*, vol. 19, no. 1, pp. 88–102, 2015.
- [31] D. Gong, J. Sun, and X. Ji, “Evolutionary algorithms with preference polyhedron for interval multi-objective optimization problems,” *Inf. Sci.*, vol. 233, pp. 141–161, 2013.
- [32] I. C. Parmee and D. Cvetkovic, “Preferences and their application in evolutionary multiobjective optimization,” *IEEE Trans. Evolutionary Computation*, vol. 6, no. 1, pp. 42–57, 2002.
- [33] I. Karahan and M. Köksalan, “A territory defining multiobjective evolutionary algorithms and preference incorporation,” *IEEE Trans. Evolutionary Computation*, vol. 14, no. 4, pp. 636–664, 2010.

- [34] J. Branke, T. Kaussler, and H. Schmeck, "Guidance in evolutionary multi-objective optimization," *Advances in Engineering Software*, vol. 32, no. 6, pp. 499–507, 2001.
- [35] G. W. Greenwood, X. Hu, and J. G. D'Ambrosio, "Fitness functions for multiple objective optimization problems: Combining preferences with Pareto rankings," in *FOGA '96: Proc. of the 4th Workshop on Foundations of Genetic Algorithms*, 1996, pp. 437–455.
- [36] T. Wagner and H. Trautmann, "Integration of preferences in hypervolume-based multiobjective evolutionary algorithms by means of desirability functions," *IEEE Trans. Evolutionary Computation*, vol. 14, no. 5, pp. 688–701, 2010.
- [37] E. Fernández, E. Lopez, S. Bernal, C. A. C. Coello, and J. Navarro, "Evolutionary multiobjective optimization using an outranking-based dominance generalization," *Computers & OR*, vol. 37, no. 2, pp. 390–395, 2010.
- [38] E. Fernández, E. Lopez, F. L. Irraragorri, and C. A. C. Coello, "Increasing selective pressure towards the best compromise in evolutionary multiobjective optimization: The extended NOSGA method," *Inf. Sci.*, vol. 181, no. 1, pp. 44–56, 2011.
- [39] B. Roy, *Multicriteria Methodology for Decision Aiding*. Kluwer Academic Publisher, 1996.
- [40] C. M. Fonseca and P. J. Fleming, "Multiobjective optimization and multiple constraint handling with evolutionary algorithms. I. A unified formulation," *IEEE Trans. Systems, Man, and Cybernetics, Part A*, vol. 28, no. 1, pp. 26–37, 1998.
- [41] K. Deb and A. Kumar, "Light beam search based multi-objective optimization using evolutionary algorithms," in *Proceedings of the IEEE Congress on Evolutionary Computation, CEC 2007, 25-28 September 2007, Singapore*, 2007, pp. 2125–2132.
- [42] —, "Light beam search based multi-objective optimization using evolutionary algorithms," in *CEC'07: Proc. of the 2007 IEEE Congress on Evolutionary Computation*, 2007, pp. 2125–2132.
- [43] U. K. Wickramasinghe and X. Li, "Integrating user preferences with particle swarms for multi-objective optimization," in *GECCO'08: Proc. of the 2008 Genetic and Evolutionary Computation Conference*, 2008, pp. 745–752.
- [44] R. Allmendinger, X. Li, and J. Branke, "Reference point-based particle swarm optimization using a steady-state approach," in *SEAL'08: Proc. of the 7th International Conference on Simulated Evolution and Learning*, 2008, pp. 200–209.
- [45] J. Molina, L. V. Santana, A. G. Hernández-Díaz, C. A. C. Coello, and R. Caballero, "g-dominance: Reference point based dominance for multiobjective metaheuristics," *European Journal of Operational Research*, vol. 197, pp. 685–692, 2009.
- [46] G. Yu, J. Zheng, R. Shen, and M. Li, "Decomposing the user-preference in multiobjective optimization," *Soft Computing*, pp. 1–17, 2015.
- [47] X. Ma, F. Liu, Y. Qi, L. Li, L. Jiao, X. D. X. Wang, B. Dong, Z. Hou, Y. Zhang, and J. Wu, "MOEA/D with biased weight adjustment inspired by user preference and its application on multi-objective reservoir flood control problem," *Soft Computing*, pp. 1–25, 2015.
- [48] A. Mohammadi, M. N. Omidvar, X. Li, and K. Deb, "Integrating user preferences and decomposition methods for many-objective optimization," in *CEC'14: Proc. of the 2014 IEEE Congress on Evolutionary Computation*, 2014, pp. 421–428.
- [49] R. Wang, J. Xiong, H. Ishibuchi, G. Wu, and T. Zhang, "On the effect of reference point in MOEA/D for multi-objective optimization," *Appl. Soft Comput.*, vol. 58, pp. 25–34, 2017.
- [50] K. Miettinen, *Nonlinear Multiobjective Optimization*. Kluwer Academic Publishers, 1999, vol. 12.

- [51] K. Li, Q. Zhang, S. Kwong, M. Li, and R. Wang, “Stable matching based selection in evolutionary multiobjective optimization,” *IEEE Trans. Evolutionary Computation*, vol. 18, no. 6, pp. 909–923, Dec. 2014.
- [52] K. Deb and R. B. Agrawal, “Simulated binary crossover for continuous search space,” *Complex Systems*, vol. 9, pp. 1–34, 1994.
- [53] K. Deb and M. Goyal, “A combined genetic adaptive search (GeneAS) for engineering design,” *Computer Science and Informatics*, vol. 26, pp. 30–45, 1996.
- [54] E. Zitzler, K. Deb, and L. Thiele, “Comparison of multiobjective evolutionary algorithms: Empirical results,” *Evolutionary Computation*, vol. 8, no. 2, pp. 173–195, 2000.
- [55] K. Deb, L. Thiele, M. Laumanns, and E. Zitzler, “Scalable test problems for evolutionary multi-objective optimization,” in *Evolutionary Multiobjective Optimization*, ser. Advanced Information and Knowledge Processing, A. Abraham, L. Jain, and R. Goldberg, Eds. Springer London, 2005, pp. 105–145.
- [56] K. Li, K. Deb, Q. Zhang, and S. Kwong, “An evolutionary many-objective optimization algorithm based on dominance and decomposition,” *IEEE Trans. Evolutionary Computation*, vol. 19, no. 5, pp. 694–716, 2015.
- [57] K. Deb and H. Jain, “An evolutionary many-objective optimization algorithm using reference-point-based nondominated sorting approach, part I: solving problems with box constraints,” *IEEE Trans. Evolutionary Computation*, vol. 18, no. 4, pp. 577–601, Aug. 2014.
- [58] R. Wang, R. C. Purshouse, and P. J. Fleming, “Preference-inspired co-evolutionary algorithms using weight vectors,” *European Journal of Operational Research*, vol. 243, no. 2, pp. 423–441, 2015.
- [59] K. Li, K. Deb, and X. Yao, “R-metric: Evaluating the performance of preference-based evolutionary multi-objective optimization using reference points,” *IEEE Trans. Evolutionary Computation*, 2017, in press.
- [60] H. Asefi, F. Jolai, M. Rabiee, and M. T. Araghi, “A hybrid NSGA-II and VNS for solving a bi-objective no-wait flexible flowshop scheduling problem,” *The International Journal of Advanced Manufacturing Technology*, vol. 75, no. 5, pp. 1017–1033, 2014.
- [61] J. Behnamian, S. F. Ghomi, and M. Zandieh, “A multi-phase covering Pareto-optimal front method to multi-objective scheduling in a realistic hybrid flowshop using a hybrid metaheuristic,” *Expert Systems with Applications*, vol. 36, no. 8, pp. 11 057–11 069, 2009.
- [62] E. Zitzler and L. Thiele, “Multiobjective evolutionary algorithms: A comparative case study and the strength Pareto approach,” *IEEE Trans. Evolutionary Computation*, vol. 3, no. 4, pp. 257–271, 1999.
- [63] J. J. Durillo, A. J. Nebro, C. A. C. Coello, J. García-Nieto, F. Luna, and E. Alba, “A study of multi-objective metaheuristics when solving parameter scalable problems,” *IEEE Trans. Evolutionary Computation*, vol. 14, no. 4, pp. 618–635, 2010.
- [64] H. Qudrat-Ullah, *Improving Dynamic Decision Making through HCI Principles*. Encyclopedia of Human Computer Interaction, 2006.